Applied Energy 242 (2019) 1074–1089

Contents lists available at ScienceDirect

Applied Energy

journal homepage: www.elsevier.com/locate/apenergy

Analysis of the high instantaneous NO_x emissions from Euro 6 diesel passenger cars under real driving conditions

Zamir Mera[a,d], Natalia Fonseca[b,*], José-María López[a], Jesús Casanova[c]

[a] University Institute for Automobile Research (INSIA), Universidad Politécnica de Madrid, 28031 Madrid, Spain
[b] Department of Energy and Fuels, Mining and Energy Engineering School, Universidad Politécnica de Madrid, 28003 Madrid, Spain
[c] Department of Energy Engineering, Industrial Engineering School, Universidad Politécnica de Madrid, 28006 Madrid, Spain
[d] Faculty of Applied Sciences, Universidad Técnica del Norte, 100105 Ibarra, Ecuador

HIGHLIGHTS

- High instantaneous NO_x represent a small percentage of observations or driving time.
- High instantaneous NO_x represent a large percentage of real-world NO_x emissions.
- Constraint of high instantaneous NO_x significantly reduce NO_x emission factors.
- Relationships between high instantaneous NO_x and several parameters were identified.
- Conditions with more probabilities of high instantaneous NO_x were identified.

GRAPHICAL ABSTRACT

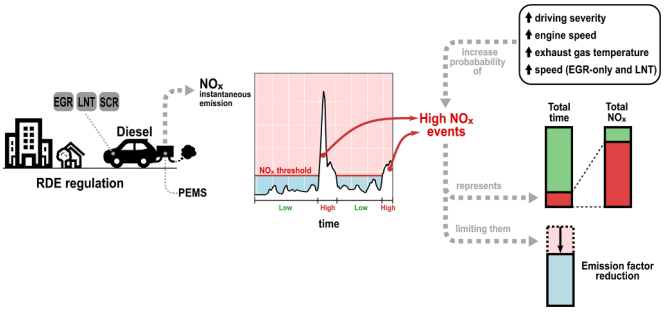

ARTICLE INFO

Keywords:
NO_x
Real driving emissions (RDE) test
Portable emissions measurement system (PEMS)
Diesel exhaust after-treatment
Passenger cars

ABSTRACT

In real-world driving, most Euro 5 and 6 diesel passenger cars exceed the nitrogen oxides (NO_x) emission limits of type approval procedure. The emission factors of the fleet of Euro 6 vehicles show high variability, irrespective of the NO_x control technology. This comprehensive study focused on the events of high instantaneous NO_x emissions produced under real driving, to assess their impact on emission factors. Additionally, the relationships of these events with different parameters measured using portable emissions measurement system (PEMS) were determined. Three Euro 6b diesel passenger cars with exhaust gas recirculation (EGR), lean-burn NO_x trap (LNT) and selective catalytic reduction (SCR) were tested based on the real driving emissions (RDE) regulation.

The results show that high instantaneous NO_x emissions represent a large amount of total NO_x emissions, although they are produced in a small percentage of driving time. A theoretical constraint of these high NO_x emissions could reduce emission factors by 30–82%. The emission of high instantaneous NO_x emissions are related to characteristic speed modes of urban, rural and motorway sections, and are primarily produced in a narrow engine speed range of approximately 700 rpm. In general, the probability of producing high

Abbreviations: CF, conformity factor; CDF, cumulative density function; DR, deviation ratio; DPF, diesel particle filter; EF, emission factor; EGR, engine gas recirculation; HES, high NO_x emissions set; LES, low NO_x emissions set; LNT, lean-NO_x trap; NEDC, new European driving cycle; NTE, not-to-exceed; PEMS, portable emissions measurement system; RDE, real driving emissions; RDE-S_i, set of valid RDE test of each vehicle *i*; RPA, relative positive acceleration; SCR, selective catalytic reduction; WLTC, worldwide harmonized light vehicles test cycle

* Corresponding author at: Department of Energy and Fuels, Universidad Politécnica de Madrid, c/Rios Rosas 21, 28003 Madrid, Spain.
E-mail addresses: zamera@utn.edu.ec (Z. Mera), natalia.fonseca@upm.es (N. Fonseca), josemaria.lopez@upm.es (J.-M. López), jesus.casanova@upm.es (J. Casanova).

https://doi.org/10.1016/j.apenergy.2019.03.120
Received 6 January 2019; Received in revised form 4 March 2019; Accepted 10 March 2019
Available online 23 March 2019

instantaneous NO_x emissions increases as the engine speed, the exhaust gas temperature or the vehicle speed is increased. Finally, regarding driving severity, speed per positive acceleration ($v{\cdot}a^+$) observations above the maximum values of the new European driving cycle (NEDC) and the world-harmonized light-duty vehicle test cycle (WLTC), have a strong probability to yield high instantaneous NO_x emissions. These findings could be useful in the design of low emission policies, optimization of NO_x control strategies, and the improvement of micro/meso emission models.

1. Introduction

NO_x emissions affect the air quality of cities and contribute to exceeding the critical loads of eutrophication in Europe [1]. During 2013–2015, a high proportion of the urban population (7–9%) in the European Union (EU) was exposed to NO_2 levels that exceeded the EU limits (Indicator CSI004) and World Health Organization guideline [2]. The transportation sector is responsible for half of NO_x emissions and 13% of other pollutants [3]. This is partially explained by the "dieselization" of the European market, with the proportion of diesel vehicles in the passenger car fleet increased from 27% to 41% between 2005 and 2015 [4]. This fleet also represents 65% of worldwide diesel vehicles sales [5].

To decrease NO_x emissions, the EU Commission reduced the type approval NO_x emission limits of diesel passenger cars from 500 to 80 mg km^{-1}. This took place between 2000 (Euro 3) and 2015 (Euro 6); however, the reduction in emissions during the last 20 years has been lower than expected [3]. In part, the problem is that light-duty vehicles have been homologated under the new European driving cycle (NEDC) [6,7]. This cycle does not reflect real-world driving due to insufficient dynamic conditions with long constant acceleration periods, smooth accelerations and low speeds [8,9]. In general, this implies that outside of NEDC conditions, emissions exceed the homologation limits. In particular, real-world driving NO_x emissions of diesel vehicles Euro 5 and 6 substantially exceed emissions limits [10]. Taking this into account, the EU Commission implemented a new homologation cycle and new procedures. From September 2017, emissions are assessed using the world-harmonized light-duty vehicle test cycle (WLTC) and the real-driving emissions (RDE) test using portable emissions measurement systems (PEMS) [11]. Currently, for the Euro 6d-TEMP, this RDE test is the not-to-exceed (NTE) type. It depends on a temporary conformity factor (CF = 2.1) set in RDE regulation, as indicated in Eq. (1). This results in an NTE limit of 168 mg NO_x km^{-1}, which must not be exceeded in either urban or total of RDE essay [12].

$$NTE_{pollutant} = CF_{pollutant}{\cdot}Euro\ \ 6\ \ emission\ \ limit \tag{1}$$

There are three main NO_x control technologies in the car market: in-cylinder technologies in concert with exhaust gas recirculation (EGR); and other two exhaust gas aftertreatments, which are lean-burn NO_x traps (LNT) and selective catalytic reduction (SCR). The EGR system has been largely implemented. It recirculates part of the exhaust gases in order to reduce the combustion temperature. However, EGR is inefficient in reducing NO_x emissions at high engine load [13,14]. For compliance of more stringent regulations, EGR can be complemented with LNT and/or SCR aftertreatments [15]. The LNT is a NO_x adsorption system that stores NO_x during lean operation conditions and regenerates under rich-engine operation. Consequently, the performance of LNT is restricted in diesel engines, and usually, it also increases fuel consumption [16,17]. This system is efficient in NO_x control at low load, although it is always physically conditioned by its storage capacity at high load [18]. SCR is the latest NO_x control technology applied to diesel passenger cars. It uses an additional source of ammonia as a precursor, resulting in a more complex aftertreatment system. SCR has demonstrated high efficiency in NO_x control (~95%), but it has operating restrictions at low temperatures [19–21].

The wide variability of NO_x emissions from Euro 6 diesel vehicles has been evidenced by studies of extensive fleets. Franco et al. [22], Ntziachristos et al. [9] determined the actual emissions level of light-duty vehicles using a large database from several sources. Yang et al. [23] tested 73 Euro 6 diesel vehicles using the WLTC cycle, and O'Driscoll et al. [24] conducted measurements of 39 Euro 6 diesel vehicles in real-world driving with PEMS. These studies identified few vehicles with NO_x emissions under Euro 6 limit of 80 mg km^{-1}, and there were high emitters that exceeded this value by up to 27 times. This is because NO_x control and aftertreatment systems have different configurations and control strategies. In addition, most of them are optimized for the NEDC cycle [23]. Another possibility is the use of improper defeat strategies [25]. This implies that the homologation process of NO_x emissions has been ineffective and it does not allow the generalization of the emissions of this diesel vehicles fleet [7]. According to Euro regulations, these vehicles will be permitted to be sold until September 2019. Therefore, it is important to know more accurately how NO_x emissions from Euro 6 vehicles approved under NEDC are produced. The impact of their emissions may be mitigated via the implementation of appropriate policies; by rethinking their emission models and recalculating their NO_x emission factors. This is not only important to Europe, given that millions of these vehicles are driven around the world, and Euro regulations have been adopted in Asia, Latin America and Oceania [9].

In the existing literature, there are several studies that analyse NO_x emissions of diesel Euro 6 vehicles with PEMS, even in essays that accomplish to a greater or lesser extent the requirements of RDE regulation. They evaluated a wide variety of aspects and had different objectives, but no study to date has analysed in detail the events of the highest instantaneous NO_x emissions, their impact on real-world emissions, and their relationship with other parameters. The aforementioned studies include the following: Luján et al. [26] used a vehicle with LNT in a single RDE route to compare the moving averaging window (MAW) and power binning (PB) methods to compute NO_x emissions. They also analysed cold start emissions. The study of Gallus et al. [27] analysed the influence of driving style and road grade in one EGR-only vehicle. Six vehicles with LNT were analysed in Kwon et al. [28]. They were compared for different driving routes, MAW and PB methods, ambient temperatures, and air conditioner use. In one of the largest studies, O'Driscoll et al. [24] measured NO_x emissions from 39 Euro 6 diesel vehicles with different aftertreatment systems in urban and motorway sections. This research compared emissions between PEMS and COPERT macro emissions models. In an extension of this study [29], NO_x emissions of diesel vehicles were compared with the emissions from gasoline and hybrid vehicles. In Korea, 17 SCR and LNT vehicles were tested in two different RDE routes by Cha et al. [30]. Among other parameters, ambient temperature was analysed. Chong et al. [31] analysed four LNT diesel vehicles in an attempt to relate vehicle specific power (VSP) values to emissions and fuel consumption. Wang et al. [32] analysed the effect of altitude up to ~3000 m in four cities in China. Triantafyllopoulos et al. [33] confirmed the potential to reduce NO_x emissions by reconfiguring EGR behaviour and implementing a SCR system. Finally, in a research report for the International Council on Clean Transportation, Franco et al. [22] briefly delineated the relationship between instantaneous NO_x emissions and binned levels of speed, acceleration*speed, road grade and exhaust gas temperature. Thus, in existing literature, high instantaneous NO_x emissions are seldom analysed.

Based on these considerations, the aim of this paper is twofold: first,

to investigate the effect of high instantaneous NO_x emissions on the vehicle's environmental performance and second, to link high instantaneous NO_x emissions to parameters of driving and operating conditions. Three Euro 6 diesel vehicles with the main NO_x control technologies were tested in a route designed in the city of Madrid, to fulfil the requirements of the RDE regulation. In order to achieve this objective, three research questions needed to be answered:

- How much do high instantaneous NO_x emissions contribute to emission factors of Euro 6 vehicles in RDE tests?
- How are high instantaneous NO_x emissions related to vehicle and engine operating conditions and driving severity?
- How are these high NO_x emissions related to different NO_x control technologies: EGR-only, LNT and SCR?

For this purpose, the events of high instantaneous NO_x emissions (emission peaks) were clustered. Then, their contributions to emission factors and their weighting in driving time were assessed. Finally, they were characterized with respect to the following parameters: vehicle speed, positive acceleration (a^+), speed per positive acceleration ($v{\cdot}a^+$), air-fuel equivalence ratio (λ) at the tailpipe, exhaust gas temperature, engine speed, and road grade. The performance and type of NO_x control technology installed in the vehicle is a determinant factor that influences the release of NO_x emissions. Therefore, all the stages of this study also assessed the differences between the tested vehicles.

This comprehensive analysis of high instantaneous NO_x emissions from real-driving tests is the main novelty of this study. Therefore, this study contributes a new perspective with respect to NO_x emissions in real-world driving from Euro 6 diesel vehicles, which have demonstrated high variance and/or bias in their NO_x emission factors. This study examines the contribution of high instantaneous NO_x in emission factors and driving time, which is important in addressing them and mitigating environmental pollution from modern diesel cars. The results also identify where these events are produced in correspondence with the parameters of driving demand; and engine and vehicle operating conditions, which is useful in the formulation of emission models, control strategies or decision-making policies.

2. Methods

2.1. Tested vehicles

Three SUV diesel passenger cars were tested. They had the following common characteristics: common rail direct injection, variable geometry turbocharger (VGT), 6-speed manual gearbox and stop-start system; all vehicles had low mileage when the testing campaign started. Also, standard commercial diesel fuel was used for all tests. The characteristics of the vehicles are shown in Table 1.

2.2. PEMS

The measurements were conducted with MIVECO-PEMS equipment, which was developed and validated at the Universidad Politécnica de Madrid (UPM) by Fonseca [34]. For exhaust gas measurements, the equipment includes two exhaust flow meters, a lambda sensor, a temperature sensor and an exhaust gas analyser. Vehicle and engine speeds were recorded from the vehicle on-board diagnosis (OBD) port. Additionally, the geographical position was obtained from a Global Positioning System (GPS), and a weather station records barometric pressure, temperature and humidity data. Specifically, this PEMS measures the concentration of NO_x with a Horiba Mexa 720 ceramic zirconium sensor, and the exhaust flow meter is Pitot tube type, as shown in Fonseca et al. [35]. The air-fuel equivalence ratio, defined as the actual air/fuel ratio over stoichiometric air/fuel ratio, was measured using a lambda sensor ETAS LA4. The speed obtained from the vehicle OBD was validated using the speed calculated from the GPS position and the speed measured by a Doppler effect sensor pointed towards the road. The PEMS power supply was derived from external batteries, so it does not directly affect engine power. Despite the increase in the mass of the vehicle, the complete PEMS system, the driver, and his co-pilot weighted approximately 190 kg. This only represented approximately 12% of the gross weight of the tested vehicles.

It was ensured that the equipment was calibrated during the entire measurement campaign, and PEMS installation procedures complied with Annex IIIA of (EU) 2017/1151 regulation [12]. Moreover, the PEMS system followed a strict verification procedure before, during and after each RDE test.

Table 1
Tested vehicles characteristics.

Vehicle Id	EGR	LNT	SCR
Manufacturer/model	Hyundai/Tucson	Honda/CR-V	Audi/Q3
Emissions type approval	Euro 6b	Euro 6b	Euro 6b
Year	2017	2017	2016
Engine displacement [L]	2.0	1.6	2.0
Power [kW]	100	88	110
Curb weight [kg]	1604	1615	1560
Mileage at start [km]	~5900	~1600	~8200
NO_x control technology	EGR	EGR + LNT	EGR + SCR

2.3. Test route

The RDE test route traversed through the city of Madrid and its surroundings. One RDE trip had a total distance of 76.5 km, and its urban, rural, and motorway sections had a distance of 23.2 km (30%), 28.8 km (38%) and 24.5 km (32%), respectively. The route was approximately a closed loop that started and ended close to the South Campus of UPM university and a trace of the route is shown in Fig. 1. The minimum altitude of the route was 519 m above sea level and it had

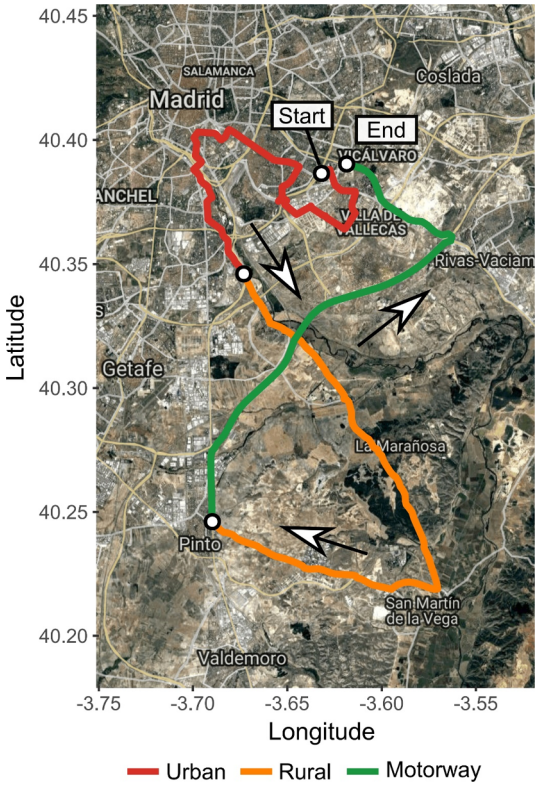

Fig. 1. RDE test route, Madrid (Spain).

a maximum positive height of 156 m. During RDE tests, the cumulative positive altitude gain for the entire trip was 828 m/100 km, which resulted in an average positive slope of 1%. The RDE test route satisfied the requirements specified in the RDE regulations.

The detailed route of each RDE section corresponds to urban section: South Campus UPM, Vallecas, Puente de Vallecas, Pacífico, Atocha, La Chopera, San Fermín y Los Ángeles, de los Rosales Avenue; rural section: De los Rosales Avenue, San Martín de la Vega (M301) road, M841 road, Pinto; and motorway section: Pinto, Andalucía (A4) highway, M50 highway, Valencia (A3) highway.

2.4. RDE test and data analysis

The PEMS observations were recorded at a frequency of 10 Hz. A given observation has the instantaneous values (at a particular time) of all parameters. Subsequently, all the parameters were revised, corrected and synchronized in the data post-treatment process to ensure that all observations in the RDE dataset had a time resolution of 0.1 s. The number of observations corresponds to the time in seconds with the ratio ten-to-one.

In order to ensure that emissions are reflected in real driving conditions, the high instantaneous NO_x emissions–in this study–were compared to other parameters without smoothing, elimination of outliers or segregation of the data [24]. Therefore, the RDE sections were discretized based on speed bins only for verification of overall trip dynamics, as is established in Appendix 7a of (UE) 2017/1151 regulation [12]. This verification guarantees that RDE tests are within regulations and reflect a normal European driving, as is demonstrated in Gallus et al. [27].

Each vehicle performed five RDE tests. This corresponded to a test campaign of 15 trips, but only 10 tests resulted valid: EGR (3), LNT (4) and SCR (3). Four tests were excluded for exceeding moderate ambient temperature conditions. Another test was discarded for exceeding ($v{\cdot}a_{pos}$) [95] limit in the verification of the overall trip dynamics, which is identified by the red[1] dot in Fig. 2. A detailed comparison between the RDE tests of this research, and RDE requirements of (EU) 2017/1151 regulation [12] is shown in supplementary material.

The dataset of all valid RDE tests for each vehicle *i*, is defined as RDE-S_i (RDE Set) in this study. The number of observations and amount of time for each RDE-S_i were: 182×10^3 observations (303 min) for EGR, 246×10^3 observations (410 min) for LNT and 178×10^3 (297 min) for the SCR vehicle. Valid RDE tests had an average trip length of 101 (sd. 2.9) min, ambient temperatures between 19.4 and 30.0 °C and averaged 24.5 (sd. 1.9) °C. RDE-S_i data summed 765 km, and a total testing time of 16 h and 50 min, resulting in ~600 thousand observations

All tests reflected normal and consistent driving and they were performed by a professional driver. Fig. 2 shows equivalent results of average speed, ($v{\cdot}a_{pos}$) [95] and RPA for all binned RDE sections. In order to achieve similar traffic and environmental conditions, the tests were performed in the morning, after rush hour during weekdays in June and July, and with moderate traffic conditions.

Cold start emissions were not analysed. RDE tests started with pre-warmed engine and emission control systems. Before the tests were conducted, the vehicle ran a pre-warming circuit of 4.9 km for about 14 min, and the engine coolant temperature exceeded 70 °C. Therefore, in this study, hot-start tests were conducted with similar requirements to (EU) 2017/1151. NO_x measurements were not corrected for air humidity to represent emissions as they occurred in real-world driving [22,24,36,37]. It is also established in Annex IIIA (EU) 2017/1151.

[1] For interpretation of color in Figs. 2, 5, 9, 11, the reader is referred to the web version of this article.

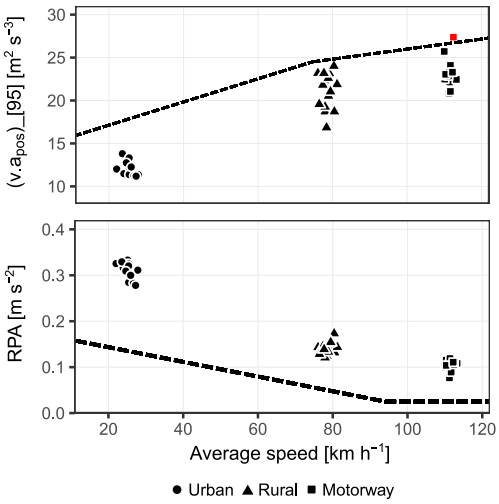

Fig. 2. Verification of overall trip dynamics of RDE tests campaign according to RDE regulation. Dashed curves indicate the excess or absence of dynamics during urban, rural and motorway driving. Upper limit corresponds to 95th percentile of $v{\cdot}a_{pos}$ values, and lower limit is determined by the relative positive acceleration (RPA) parameter.

2.5. Cumulated NO_x emissions

Instantaneous NO_x emissions (in mg s^{-1}) are obtained from instantaneous exhaust gas flow and instantaneous NO_x concentration, which were measured by the exhaust flow meter and the gas analyser, respectively. The cumulated NO_x emissions (in mg) is the integral of the instantaneous emissions over the time, and it represents the total mass of NO_x emitted. Since the data was synchronized at a sampling frequency of 10 Hz, the cumulated NO_x emissions of any dataset *j*, is given as:

$$m_j = \sum_n \dot{m}{\cdot}\Delta t \tag{2}$$

where $\dot{m}$ is the instantaneous NO_x emission (in mg s^{-1}) of each observation of the dataset *j*, *n* is the number of observations of the dataset and Δt is the sampling time, equal to 0.1 s.

2.6. Emission factors

The raw distance-specific emission factor (in mg NO_x km^{-1}), for RDE section *k*, was computed as:

$$EF_k = \frac{m_k}{s_k} \tag{3}$$

where m_k is the cumulated mass emission of section *k* for the travelled distance s_k (in km). Subscript *k* is *u, r,* and *m* for the urban, rural and motorway RDE sections, respectively.

For the entire RDE tests, the weighted distance-specific emission factor establishes fixed distance proportions for each RDE section. It was computed as:

$$EF_w = 0.34{\cdot}EF_u + 0.33{\cdot}EF_r + 0.33{\cdot}EF_m \tag{4}$$

where the weightings of (EU) 2017/1151 regulation are taken into account. This corresponds to proportions of 34% (urban), 33% (rural) and 33% (motorway). See supplementary material for detailed results of emission factors.

In this study, the dimensionless term emission factor ratio ($EF\varphi = EF_k/EF_w$) was used to compute the mean contribution of each section to the weighted emission factor.

In order to compare emission levels of section *k* with respect to regulations, the dimensionless term deviation ratio (DR) was used [24,38,36,39]

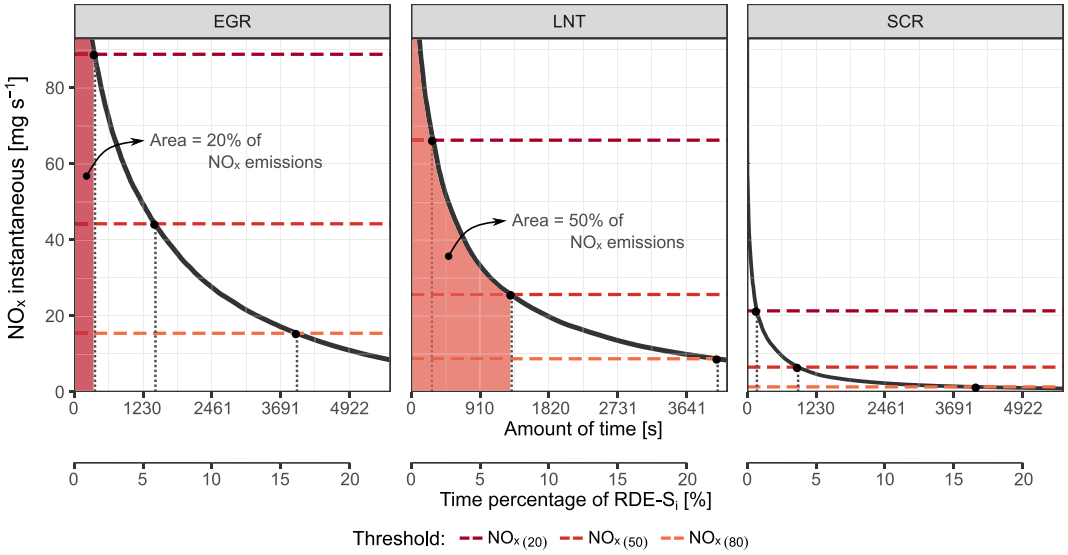

Fig. 3. Determination of High emissions sets (HES). The area under the curve represents the cumulative NO_x emissions. The areas are trimmed at the top to improve visualization.

$$DR_k = \frac{m_k/s_k}{ES} \quad (5)$$

where ES is the emission standard limit of 80 mg NO_x km^{-1} imposed for Euro 6 vehicles.

2.7. Determination of high NO_x emissions sets (HES)

A "high" emissions set (HES) is defined as the dataset with observations of the highest instantaneous NO_x emission of any RDE-S_i (all valid RDE tests for each vehicle *i*). Cumulated emissions of HES calculated using Eq. (2), represents a desired percentage of RDE-S_i total emissions. To determine HES, the instantaneous NO_x emissions of each vehicle were sorted in decreasing order; then, cumulated emissions were computed starting with the maximum instantaneous NO_x emission until the desired percentage of total emissions was reached. Thus, for each vehicle there could be multiple HES-y, where "y" is the percentage of cumulated emissions. The corresponding complementary set of "low" emissions is LES-(100-y). Another outcome of this process is the threshold $NO_{x(y)}$ (in mg s^{-1}). It is the minimum instantaneous emission (lower limit) of HES-y, and it is useful to classify HES observations. Thus, observations with NO_x values equal to or greater than $NO_{x(y)}$ are HES-y, and observations below the $NO_{x(y)}$ value belong to LES-(100-y). For instance, as shown in Fig. 3, HES-20 represents the set of observations with the highest instantaneous NO_x emissions, whose cumulated emissions are 20% NO_x of RDE-S_i. This corresponded to instantaneous NO_x emissions over the threshold of 88.8, 66.2 and 21.3 mg s^{-1} for EGR, LNT and SCR vehicles; in addition, it corresponded to 1.5, 1.6 and 0.7% of the total time, respectively. The observations below that threshold belong to LES-80. As a result of this classification procedure, every percentage of time and cumulated emissions of HES are shown in Fig. 5 and Table 2.

2.8. Impacts of high NO_x emissions

HESs were used to evaluate the impact of high NO_x emissions on the driving time and the emission factors. The amount of time was obtained directly from the process of determination of HES, and it was compared for each vehicle to the total time of the RDE tests (RDE-Si). To assess the impact of high NO_x on emission factors, NO_x thresholds were used as maximum values of instantaneous NO_x emissions of RDE tests. Thus, the observations that belong to HES were replaced by their respective NO_x threshold. Then, emission factors were recalculated as noted in Section 2.6. These new reduced emission factors were compared to those of the RDE tests.

2.9. Analysis of parameters

The instantaneous data of analysed parameters were derived from PEMS. They were related to vehicle and engine operating conditions and/or driving severity, see Fig. 4. Firstly, the parameters of acceleration, speed and road grade characterize vehicle operating conditions, as their variability depends mainly on traffic conditions and road infrastructure. However, the parameters of engine speed, exhaust gas temperature and air-fuel equivalence ratio (λ) characterize engine operating conditions; their variability depends on engine type, fuel, engine control strategies, among other factors. In this study, the air-fuel equivalence ratio and exhaust gas temperature were measured at the tailpipe (downstream of engine and NO_x control technologies). These parameters are "paired" to variables that were considered by D'Ambrosio et al. [40] in a semi-empirical NO_x in-cylinder model. The variables were maximum in-cylinder burned gas temperature during the combustion of the main pulse, the stoichiometric ambient gas-to-fuel ratio[2] and the engine speed, in addition to the mass of injected fuel and injection pressure.

Vehicle and engine operating conditions are not independent, and they are both interrelated with the driving style. Driving style was analysed using different driving parameters such as RPA, mean a^+, $v{\cdot}a^+$, and engine speed [42,22,27]. With respect to normal driving, aggressive driving increases the demand for engine power by increasing engine speed, which leads to increased acceleration and speed of the vehicle. Similarly, driving severity increases the demand for engine power due to an "aggressive" speed-time profile. In this study, speed per positive acceleration ($v{\cdot}a^+$), which is an approximation of instantaneous VSP [22], was used to compare the driving severity of NEDC and WLTC cycles with RDE tests.

A descriptive statistical analysis was performed to find relationships between high instantaneous NO_x emissions and the analysed

[2] It is also called "unburned gas-to-fuel ratio", which reflects the mass of in-cylinder unburned gas that is required for stoichiometric combustion per unit of fuel mass. It depends of the mass of air, the amount of trapped EGR mass and residual gas. If the oxygen concentration in the unburned gas tends to that of fresh air, the unburned gas-to-fuel ratio is equal to stoichiometric air-to-fuel ratio. See [40,41].

Table 2
NO_x thresholds and percentage of time of high emissions sets.

High emissions set	Cumulated NO_x [%]	EGR		LNT		SCR	
		NO_x threshold [mg s^{-1}]	Time [%]	NO_x threshold [mg s^{-1}]	Time [%]	NO_x threshold [mg s^{-1}]	Time [%]
HES-20	20	88.8	1.5	66.2	1.6	21.3	0.7
HES-50	50	44.2	5.9	25.6	7.3	6.5	3.7
HES-80	80	15.4	16.2	8.7	22.3	1.3	16.7

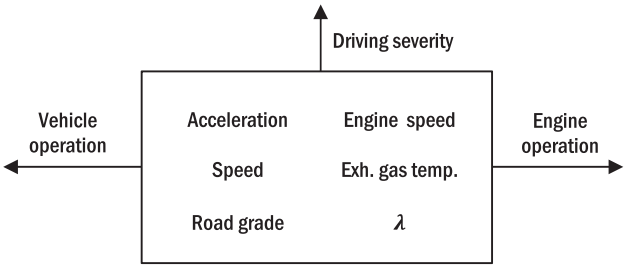

Fig. 4. Relationship between operating conditions and analysed parameters.

parameters. Two methods were applied for the analysis.

For each parameter, the first method compares the number of observations (frequency distributions) of high NO_x emissions (HES) with respect to the total number of observations (frequency distributions of RDE-S_i).

The frequency distributions of HES are affected by RDE test conditions, i.e. HES frequency distributions are likely to be greater in RDE test values with a high occurrence (high frequency). Therefore, the second method exhibits conditional probabilities: the proportion of the number of observations for high NO_x emissions compared to the number of observations of RDE-S_i. In this way, the conditional distribution illustrates the conditions whereby high NO_x emissions are present, regardless of the test conducted. Strictly speaking, it could be computed using the conditional probability mass function of $X = x$, given $Y = y$, using the equation:

$$g(x|y) = \frac{f(x, y)}{f_Y(y)} \tag{6}$$

For any analysed parameter, X and Y are discrete random variables. X = {0, 1}, where 1 means belonging to HES, and 0 indicates does not belong. $Y = \{a_1, a_2, \ldots, a_n\}$, where a is the count of the parameter in each bin of RDE-S_i data (discretized in n bins). In Eq. (6), $f(x, y)$ is the joint probability distribution, and $f_Y(y)$ corresponds to the marginal probability distribution. Thus, plots with conditional probability mass function of $X = 1$, given RDE-S_i data are shown for each analysed parameter.

The plots of frequency, conditional and density distributions were smoothed to improve visualization. In this regard, default settings in R were used to determine a Gaussian kernel density estimator. The methods used by R algorithms are explained in Venables and Ripley [43]. The bandwidth was adjusted to half of the default value to show the transitions between high/low-frequency data distribution. Due to the difference in the dataset length of RDE-S_i for each vehicle, all plotted frequency distributions were normalized to 1000 observations (RDE-S_i = 1000 observations).

3. Results and discussion

For the main purposes of this study, sets of observations with the highest instantaneous NO_x emissions: HES-20, HES-50 and HES-80 were considered. For each vehicle, they represent 20%, 50% and 80% of cumulated NO_x emissions of RDE tests. To answer the research questions, these HES were analysed using two approaches:

- Section 3.1: Emission factors, cumulative percentage of emissions and percentage of time were compared to determine the overall impact of high instantaneous NO_x emission in real-driving.
- Section 3.2: The relationships between the analysed parameters, the high instantaneous NO_x emissions and the NO_x control technologies were determined.

3.1. Impacts on driving time and emission factors

3.1.1. Impact of high instantaneous NO_x emissions on driving time

Fig. 5 shows (as stated in Section 2.7) the high emissions sets: HES-20, HES-50 and HES-80 for each vehicle. Every HES-y is characterized in the figure by: the percentage of cumulated NO_x (dot-dashed vertical lines). Every line intersects with three instantaneous NO_x emissions (black lines) values, which represent the NO_x threshold for each vehicle. Similarly, every vertical line intersects with three percentage of time (blue lines) values. Table 2 includes a summary of the numerical results. Fig. 5 also shows low emissions sets LES-(100-y) complementary to each HES-y.

An interesting finding is that observations with high instantaneous NO_x emissions, represented by HES, account for a large amount of cumulated emissions in a small percentage of time (or percentage of observations). For example, 80% of the total emissions (HES-80) were cumulated in approximately 20% of the total time, namely, 16.2, 22.3 and 16.7% for EGR, LNT and SCR vehicles, respectively. The remaining 20% of the total emissions (LES-20) were generated in ~80% of the total time. Chong et al [31] determined that 40% of the total NO_x emitted during the entire driving test occurred in 7.3% of the total driving time.

SCR vehicle reduced instantaneous NO_x emissions in the entire range of possible emission values. In Fig. 5, the instantaneous emissions (black) and time (blue) curves of HES have similar profiles for the three tested vehicles, but the EGR instantaneous emissions are not only higher than that of LNT but also much higher than that of SCR emissions. Therefore, HES threshold values of instantaneous NO_x have the same tendency, as shown in Table 2.

The upper limit of the time percentage curves (blue in Fig. 5) shows that there were no NO_x emissions during a substantial amount of time: 12% (EGR), 13% (LNT) and 21% (SCR). This corresponds to the stop periods ($v < 1$ km h^{-1}). RDE tests resulted in average stop periods of 16.6% (EGR), 18.4% (LNT) and 17.7% (SCR). Under these conditions, unless the engine is turned off by the stop-start system, there is a low NO_x concentration and a low exhaust gas flow.

The time share by RDE sections in Fig. 6 shows that observations of high emissions of EGR and LNT vehicles were mainly in rural and motorway sections of the route. However, SCR system reduced its emissions, and this vehicle produced its relatively high emissions in rural and mostly in urban sections. EGR vehicles exhibited a regular behaviour between HES sets. LNT and SCR systems are more dependent on the particular conditions of each RDE section, such as exhaust gas temperatures and flow, and engine load. Finally, as NO_x thresholds decrease, i.e. transitioned from HES-20 to HES-80, the urban section increases the percentage of time with high instantaneous NO_x. This is more evident for the SCR vehicle, which reached 56% of the high NO_x emissions in the urban region for HES-80. The percentage of time (or

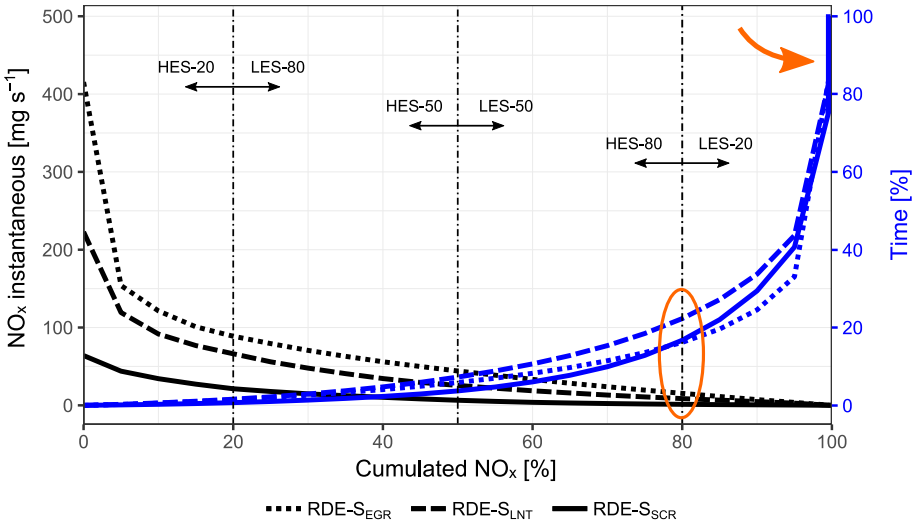

Fig. 5. High emissions sets (HES) with corresponding low emissions sets (LES) for RDE tests data of each vehicle (RDE-S_i). Curves represent NO_x instantaneous emissions (black) and percentage of time (blue). (For interpretation of the references to color in this figure legend, the reader is referred to the web version of this article.)

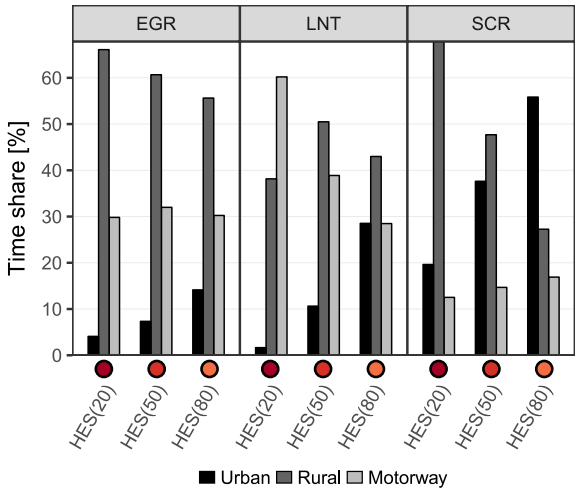

Fig. 6. Percentage of time of high instantaneous NO_x emissions in every RDE section.

percentage of observations) is useful in determining where high instantaneous emissions are produced, but emission factors of light-duty vehicles are usually based on distance, therefore; they are also dependent on speed. The impact on emission factors is discussed in the following section.

3.1.2. High instantaneous NO_x emissions and emission peaks

Fig. 7 shows that high NO_x emissions are short events that occur throughout the trip. Therefore, cumulated emissions are mainly represented by these short time events. For each vehicle, this figure contains raw instantaneous NO_x emissions for an RDE test with the maximum emission peak of NO_x. It also represents vehicle speed and the values of NO_x thresholds ($NO_{x(y)}$) for each high emission set. By way of illustration, the LNT vehicle had the event of maximum NO_x emission between ~4700 and ~4710 s. This peak surpasses the three NO_x thresholds, so observations of this event belong to the three high emissions sets: HES-20, HES-50 and HES-80. Previous studies noted that high emissions correspond to emission peaks, which are usually smoothed or treated as outliers. These high emissions also increase the emission factors, mainly in conditions of high dynamics [44,24]. In the Fig. 7, the maximum peaks of EGR and LNT vehicles match with strong acceleration at high speeds. On the other hand the emission peaks and HES threshold are significantly reduced by the vehicle equipped with the SCR system.

3.1.3. Impact of high instantaneous NO_x emissions on emission factors

Fig. 8 shows the average emission factors as bars with inclined pattern filling. They were computed with the methods of Section 2.6 to obtain raw and weighted distance-specific emission factors. EGR and LNT vehicles had the highest emission factors for any section or test (DR_k = 5.1–13.0). Therefore, they significantly exceeded the Euro 6 type approval limit (80 mg NO_x km^{-1}) and NTE Euro 6d-TEMP limit. On the other hand, the emission factors of the SCR vehicle was kept under the NTE limit and sometimes under the Euro 6 limit, with DR_k = 0.6–1.6. The results in Yang et al. [23] showed that vehicles with these three NO_x control technologies accomplished with Euro 6 limits in the NEDC cycle, however, they did not in the WLTC cycle. In the case of the WLTC cycle, vehicles with SCR presented fewer NO_x emissions factors compared to the vehicles with EGR-only and LNT systems. In other studies with PEMS, May et al. [45], Triantafyllopoulos et al. [33], Weiss et al. [36] have also shown that SCR systems have the potential to reduce NO_x emissions. The extensive research of O'Driscoll et al. [24] found that SCR and LNT technologies were able to meet the Euro 6 standard, but EGR alone was not. Recent studies show that the EGR system could improve the trade-off between NO_x emissions and fuel consumption in diesel engines by the use of asymmetric twin-scroll turbocharging [57], and improve even more its performance using two EGR circuits [58]. Nonetheless, these results and the current stringent legislations emphasizes the need to use NO_x aftertreatment systems to satisfy Euro 6 and futures emission limits in real-world driving.

The SCR tested vehicle is efficient at reducing NO_x emissions, particularly in the motorway section. Similar trends for the comparison of SCR vehicles in urban and motorway sections were found in O'Driscoll et al [24]. Although the SCR vehicle had low emission factors, its emission factor ratios show that urban ($EF\varphi$ = 1.40) had a much greater contribution compared to motorway ($EF\varphi$ = 0.50), as highlighted in Table 3. This resulted in emission factors in the following order: $EF_u > EF_w > EF_m$, with average DR values for urban (1.6), weighted (1.1) and motorway (0.6), as the lowest emission factor in the study. However, for EGR and LNT vehicles, their emission factor ratios show that rural and motorway ($EF\varphi$ = 0.93–1.50) contributed more than urban ($EF\varphi$ = 0.58–0.85). Their motorway emission factors were similar to the weighted emission factors, and greater than the urban emission factors, namely $EF_m \approx EF_w > EF_u$. Thus, worse-NO_x-reducers (EGR and LNT) vehicles had average deviation ratios for motorway (8.0, 7.7), weighted (8.7, 7.4) and urban (5.1, 6.3). At the tailpipe, the measured emissions are related to the overall environmental performance of the vehicle. However, from the perspective of the engine, tailpipe emissions are related to NO_x control system performance, and vehicles were defined as better or worse NO_x-reducer.

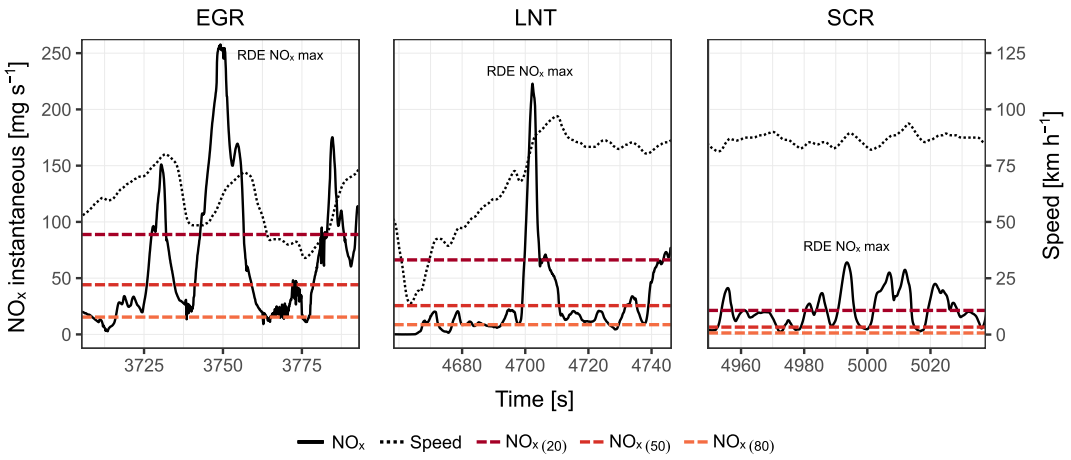

Fig. 7. Raw PEMS data of instantaneous NO_x emissions and vehicle speed. Horizontal dashed lines show the different thresholds of each vehicle and each high emission set.

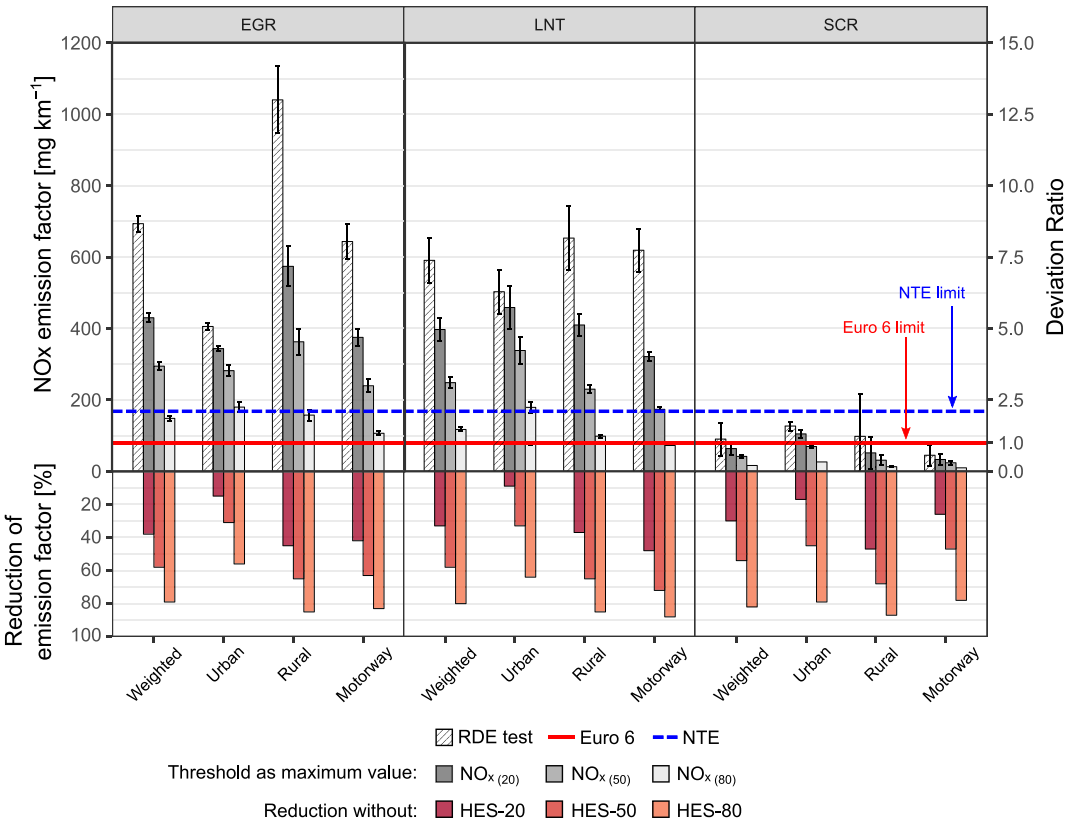

Fig. 8. Comparison of tested and reduced emission factors. Weighted and raw distance-specific emission factors from tests (bars with inclined pattern filling). In grey scale, the reduced emission factors based on the NO_x thresholds as maximum values of instantaneous NO_x emissions. The bars below the horizontal axis represent the reduction percentage of emission factors of the upper bars. The error segments represent ± 1 sd. NTE limit corresponds to 168 mg NO_x km^{-1} of Euro 6d-TEMP (CF = 2.1).

Fig. 8 also shows the reduced emission factors by the NO_x thresholds, and their percentage of reduction. It should be noted that observations with emission peaks were not removed, but they were constrained to their threshold value to determine the impacts of high NO_x on the emission factors, as is explained in Section 2.8. Depending on HES analysed, weighted emission factors were reduced by 30–38% for HES-20, 54–58% for HES-50, and 79–82% for HES-80. It shows the big impact of the highest emissions, e.g. HES-20, which represents only 20% of the total emissions in a small percentage of driving time (0.7–1.5%).

Comparing RDE sections, worse-NO_x-reducers (EGR and LNT) vehicles had a greater impact on rural (reduction of 37–85%) and motorway sections (reduction of 42–88%). SCR exhibited a similar reduction percentage for the rural section (47–87%). The lowest impact was always on the urban section for the three vehicles; however, the SCR vehicle showed higher percentages of reduction than the others, with a reduction of up to 80%. To accomplish with normative, Euro 6 limits must be achieved in urban and entire RDE tests. Therefore, SCR vehicles could satisfy Euro 6 limit by reducing NO_x emissions of HES-50, which would result in $DR_u = 0.9$ and $DR_w = 0.8$. However, EGR and LNT vehicles could almost satisfy the NTE limit by reducing HES-80, both with $DR_u = 2.2$, and DR_w of 1.5 and 1.9, respectively.

Table 3
NO_x emission factors ratio (EFφ).

EFφ	EGR	LNT	SCR
EFu / EFw	0.58	0.85	1.40
EFr / EFw	1.50	1.11	1.08
EFm / EFw	0.93	1.05	0.50

Grey cells are sections where emissions are less than the weighted emission factors.

These results imply that NO_x emission factors could be substantially reduced if NO_x emission control and aftertreatment systems are effectively applied to these emission peaks. Therefore, it is relevant to investigate the conditions where these high emission events occur, so this study also performed an analysis of HES with respect to other parameters. The findings are discussed in the following section.

3.2. Analysis of parameters

3.2.1. Vehicle speed on RDE test

The vehicle speed profiles of the RDE tests were similar and this allowed them to be compared. For the RDE-S_i of each vehicle, Fig. 9a and b show similar cumulative and probability density functions of the speed (blue lines). RDE-S_i average speeds were: 45.4 km h^{-1} for EGR, 44.8 km h^{-1} for LNT, and 46.3 km h^{-1} for SCR. Fig. 9a, also shows the cumulative density function (merged vehicles) for urban, rural and motorway sections. It is observed that each section has a well differentiated speed profile. Specifically, speed ranges were between the 5th and 95th percentiles values of 0–48 km h^{-1} for urban and 20–89 km h^{-1} for rural sections, while speeds over 75 km h^{-1} (5th percentile) were measured for motorway sections. This resulted in RDE test mode (Mo) values of $Mo_{urban} \approx 44$ km h^{-1}, $Mo_{rural} \approx 87$ km h^{-1}, and $Mo_{motorway} \approx 121$ km h^{-1}, as shown in Fig. 9b.

WLTC and NEDC cycles are also plotted in Fig. 9a and b. It is observed that the RDE speed profiles were more similar to the WLTC cycle than the NEDC cycle; although the WLTC cycle does not have the same speed mode values as the RDE speed distribution.

For the three tested vehicles, Fig. 10a compares RDE tests (RDE-S_i) frequency distributions (grey area) and frequency distribution of the high emissions sets previously defined: HES-80, HES-50 and HES-20. Frequency distribution curves have been normalized to facilitate an easier comparison. As a result, Fig. 10a shows that high instantaneous NO_x emissions were mainly generated in the modal speed values of each RDE section (urban, rural and motorway). Surprisingly, these modes occurred at speeds that were close to the speed limits of urban and motorway sections. Speed limits are a very important factor in driver's speed selection and there is a tendency for the coordination of speed between drivers to maintain a uniform running speed [46,47]. Therefore, high NO_x emissions in real-world driving or in RDE tests will occur with a high frequency at speed values related to traffic regulations and/or design of the RDE route. Although the speed limits of the tested RDE route (in Madrid, Spain) were 50 km h^{-1} for urban and 120 km h^{-1} for highway, RDE regulation in [12] established speed limits of 60 km h^{-1} for urban and 145 km h^{-1} for motorway.

Fig. 10b, shows the probability of producing high NO_x emissions regardless of the RDE tests frequency distribution. EGR and LNT vehicles were more likely to emit high instantaneous NO_x at high speed. These vehicles increase the conditional probability of high emissions as speed increases, so that their curves show a negative asymmetry. In Fig. 10a, EGR and LNT vehicles have a higher frequency of HES observations in high speed modes (rural and motorway) than the low speed mode (urban), although the opposite pattern for RDE distribution is evident. According to Myung et al. [17], Weiss et al. [37], these NO_x control technologies reduce performance during high-engine-load driving due to: limitation of gas recirculation in EGR and limitation of storage capacity in LNT systems.

Compared with EGR and LNT vehicles, the SCR vehicle showed different patterns of frequency and conditional distributions for HES observations. In Fig. 10a, the SCR vehicle exhibits a higher frequency of HES observations for urban and rural modes, with a considerable reduction in the frequency of motorway speed mode. The highest NO_x peaks (HES-20 and HES-50) for speeds above 110 km h^{-1} are not present, while Fig. 10b shows a slight increase of the HES-80 probability at low speeds (approximately 25 km h^{-1}). The patterns of the SCR vehicle agrees with the effective reduction of emission factors exhibited by this vehicle, specifically in the motorway section. According to Yang et al. [18], on average, the SCR system performs better than EGR-only and LNT systems in high speed ranges. This was also evidenced in extra-high-speed sub-cycles of WLTC in Yang et al. [23].

3.2.2. Positive acceleration (a^+) and speed per positive acceleration ($v{\cdot}a^+$)

Fig. 11a and b show cumulative density functions (CDF) for positive acceleration (a^+) and vehicle speed per positive acceleration ($v{\cdot}a^+$) for RDE tests of each vehicle (RDE-S_i). It is observed that these two functions are similar for all the vehicles (black lines). The motorway section (dotted grey line) had lower records of a^+ and higher records of $v{\cdot}a^+$ compared to the other RDE sections. Conversely, the urban section (continuous grey line) showed an opposite pattern to the motorway section.

Real-world driving tests had $v{\cdot}a^+$ values over the maximum values of NEDC and WLTC cycles, particularly in rural and motorway sections. The dot-dashed red line ($v{\cdot}a^+ = 9.2\ m^2\ s^{-3}$) represents the maximum value of $v{\cdot}a^+$ in the NEDC cycle, and it defines the threshold between "mild" and "strong" driving severity according to [22]. Similarly, the dot-dashed blue line ($v{\cdot}a^+ = 20.1\ m^2\ s^{-3}$) represents the maximum value of $v{\cdot}a^+$ in the WLTC class 3b cycle. Thus, in Fig. 11b it is observed

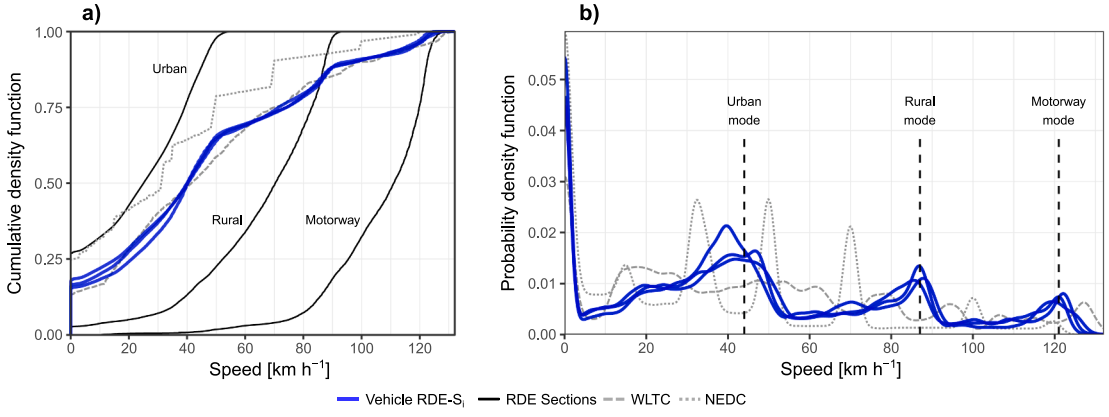

Fig. 9. Vehicle speed distributions for NEDC, WLTC and RDE tests of each vehicle (RDE-S_i) (a) cumulative density function (b) probability density function.

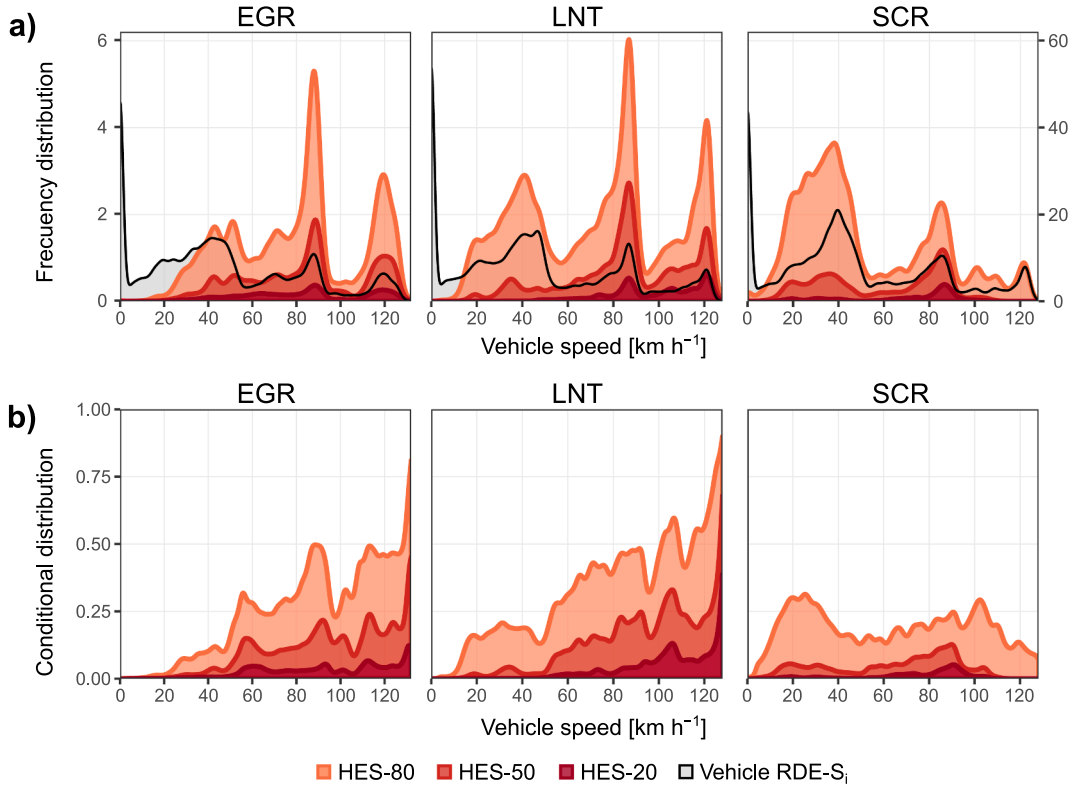

Fig. 10. Vehicle speed distributions (a) frequency distribution values of high emission sets (HES) on the left axes, and RDE tests (RDE-S_i) on the right axes. Frequency distributions are normalized, RDE-S_i = 1000 observations (b) conditional probability distribution of HES.

that 15–18% of the acceleration time for the entire RDE tests coincided with "strong" driving. This corresponds to 31–34% of the acceleration time of the motorway, 25–27% of rural, and 4–7% of urban sections. It is also observed that only 2–3% of the RDE total acceleration time had $v{\cdot}a^+$ values above the threshold of the WLTC cycle.

Fig. 12a and b show a^+ and $v{\cdot}a^+$ boxplots for high NO_x emissions sets (HES-20, HES-50 and HES-80) and RDE-S_i. High emissions have a positive correlation with high $v{\cdot}a^+$ values for all vehicles. In the case of EGR and LNT vehicles, these $v{\cdot}a^+$ values are related to a strong acceleration at elevated speeds. This is clearly illustrated in the emission peaks of the raw data (Fig. 7), considering that the emission factors and HES speed observations were relevant in rural and motorway sections for EGR and LNT vehicles. As stated by Heijne et al. [44] higher speeds and higher dynamics increases NO_x emissions in diesel Euro 6 vehicles. It was also stated by Costagliola et al. [48] about high instantaneous emissions of two Euro 5 EGR-only diesel vehicles. In Chong et al. [31] high NO_x emissions of Euro 6 LNT diesel vehicles are attributed to high speed, high acceleration, low EGR mass flow rate, and regeneration of the diesel particle filter (DPF).

Even though the SCR vehicle reduced emissions (especially on the motorway), its relatively high emissions were produced mostly in the urban and rural sections. With changing speeds, these sections usually reflect high a^+ values. In Fig. 12a, the SCR vehicle shows a positive correlation of high NO_x emissions with a^+ (it is less evident for the EGR and LNT vehicles). This is consistent with the observations of O'Driscoll et al. [24] who noted high NO_x emissions in sub-trips with high RPA at low speeds.

For $v{\cdot}a^+$, Fig. 13 shows the probability of HES observations independent of the RDE-S_i frequency distribution. It is observed that the three vehicles have higher conditional probabilities for high NO_x emissions as $v{\cdot}a^+$ increases, although the RDE-S_i frequencies are left shifted. The conditional probability is more relevant when $v{\cdot}a^+$ is

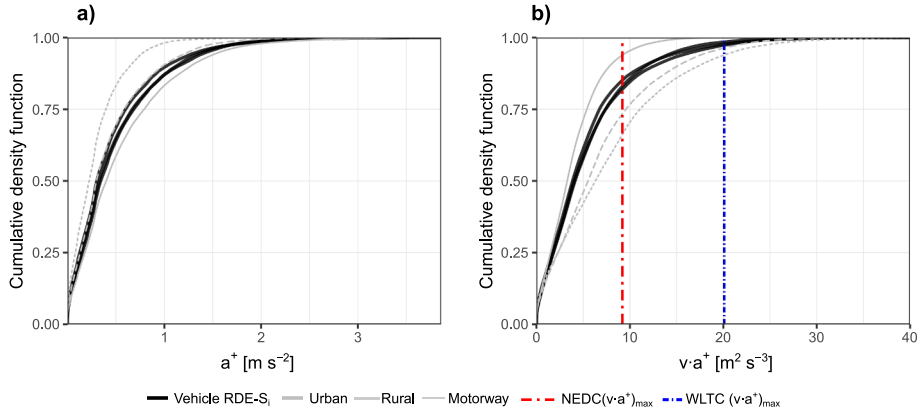

Fig. 11. Cumulative density functions of RDE tests of each vehicle (RDE-S_i) (a) positive acceleration (a^+) (b) vehicle speed per positive acceleration ($v{\cdot}a^+$), and maximum values for NEDC and WLTC cycles.

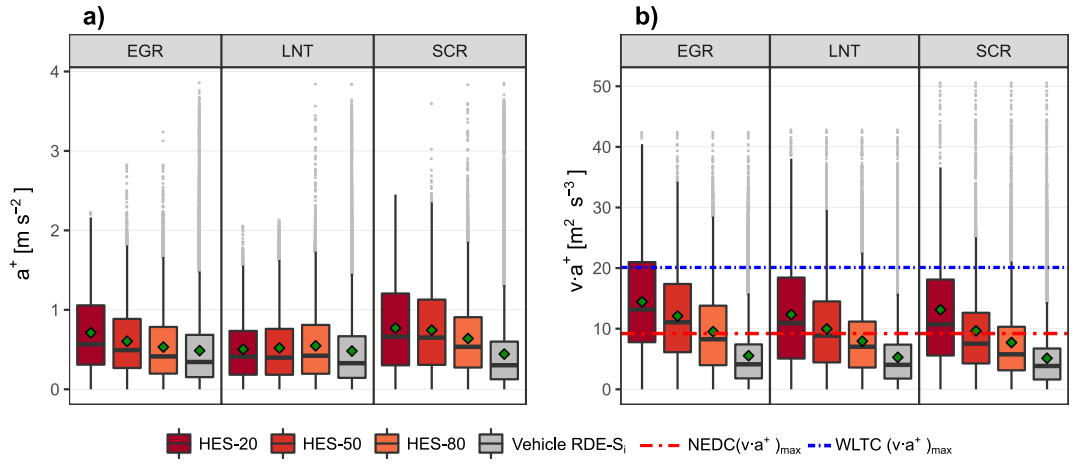

Fig. 12. Boxplots for high emissions sets (HES) and RDE tests (RDE-S_i) (a) positive acceleration (a^+) (b) vehicle speed per positive acceleration ($v{\cdot}a^+$). The dot-dashed lines indicate the maximum $v{\cdot}a^+$ values of NEDC and WLTC cycles. Central line in boxplot = median, green rhombus = mean. (For interpretation of the references to color in this figure legend, the reader is referred to the web version of this article.)

higher than the "strong" driving conditions of NEDC and this probability is much larger when $v{\cdot}a^+$ surpasses the maximum value of the WLTC cycle. For example, "strong" $v{\cdot}a^+$ values had minimum conditional probability for HES-80 emissions of 45%, 62% and 34% for EGR, LNT and SCR vehicles, while $v{\cdot}a^+$ values over maximum $v{\cdot}a^+$ value of WLTC (blue line) had at least 90%, 93% and 70% probability of being HES-80 emissions, respectively.

Therefore, in this study it is verified that parameter $v{\cdot}a^+$ is a robust indicator for the assessment and prediction of high instantaneous NO_x emissions for the three NO_x control technologies. This hypothesis could be assessed in a wide-ranging vehicle fleet. An important consequence is that speed reduction policies can lead to NO_x emissions reduction as long as they do not increase driving dynamics i.e. allowing fluid traffic with constant speed and limiting stops or aggressive acceleration.

3.2.3. Air–fuel equivalence ratio (λ) and exhaust gas temperature

The thermal NO_x formation is described by the Zeldovich mechanism [49]. It is well-known that high NO_x emissions are correlated to high exhaust gas temperatures, due to the thermal formation of NO_x during the combustion process in the engine's cylinder. Under these conditions, the flame temperature is high and there is excess oxygen during the flame diffusion process in diesel engines [50,19]. Therefore, it is usual for diesel engines to generate more NO_x in the motorway and rural sections because higher engine loads are required [51,27]. Under these conditions, an increase in fuel injection and a reduction of the air-fuel equivalence ratio occurs[50,52]. All the tested vehicles had stop-start systems, therefore the air-fuel equivalence ratio and exhaust gas temperature were not analysed during engine-off periods (engine speed $<$ 50 rpm).

The air-fuel equivalence ratio was measured at the tailpipe. Box plots for HES and RDE tests are shown in Fig. 14. It was determined that most of the high instantaneous NO_x emissions occurred under slightly lean-mixture burn conditions ($1 \lesssim \lambda \lesssim 1.5$) as measured at tailpipe. As shown in this figure, the HES of three tested vehicles had at least 75% of their lowest observations (75th percentile) for HES-20 and HES-50 within that range, and at least 50% of the lowest observations (median) for HES-80 also in this range. In comparison, RDE-S_i boxplots revealed that more than 75% of the observations with the highest values exceeded that range ($\lambda > 1.5$). The engines of the tested vehicles frequently operated with a slightly lean mixture ($1 \lesssim \lambda \lesssim 1.5$) in the rural and motorway sections due to the higher power demand. These sections were within that range approximately 30–35% of the time, while the urban section had only 10% of the time under this condition. These results are consistent with the expectations upstream of the after-treatment systems and in combination with the other measured parameters, could form robust predictors for the identification of high instantaneous NO_x emissions.

The cumulative density functions of the tailpipe exhaust gas temperature are shown in Fig. 15. It is observed that the exhaust gas temperature of the three tested vehicles (black line) had similar profiles. Clearly, the temperatures for the motorway section (average 133–151 °C) are greater than that of the urban section (average 69–82 °C).

Fig. 15 also shows that the CDF curves of HES-20, HES-50 and HES-80 have higher temperature values than RDE-S_i distributions. The tested vehicles showed different association patterns between high NO_x

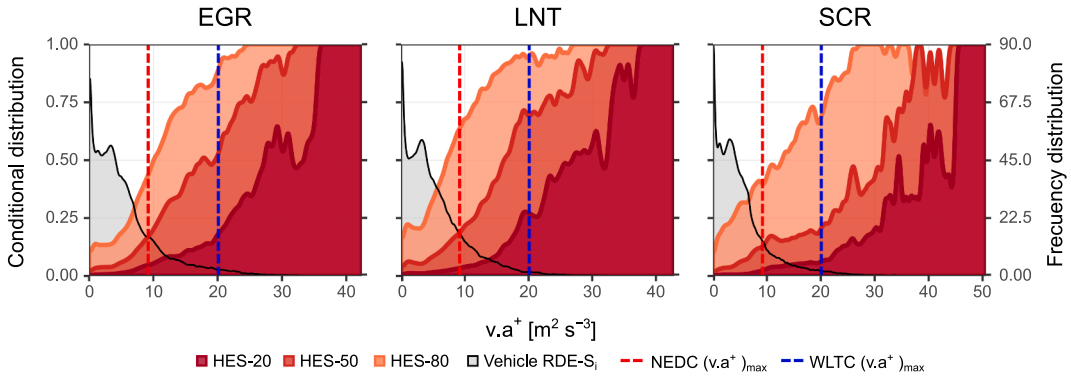

Fig. 13. $v{\cdot}a^+$ conditional probability for high emission sets (HES) on the left axes. On the right axes, grey area represents $v{\cdot}a^+$ frequency distribution of RDE tests (RDE-S_i); normalized as RDE-S_i = 1000 observations. The dashed lines indicate the maximum $v{\cdot}a^+$ values of NEDC and WLTC cycles.

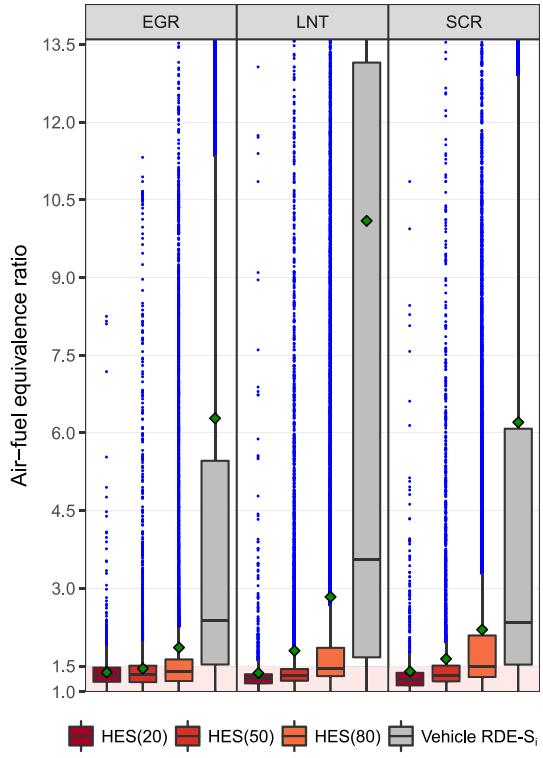

Fig. 14. Boxplot comparison of tailpipe air-fuel equivalence ratio (λ) for High emissions sets (HES) and RDE tests (RDE-S$_i$); central line in boxplot = median, green rhombus = mean, y axis is trimmed at the top to improve visualization. (For interpretation of the references to color in this figure legend, the reader is referred to the web version of this article.)

emissions and exhaust gas temperatures. Worse-NO_x-reducers (EGR and LNT) vehicles had most HES observations related to "high" exhaust gas temperatures (≳75 °C). EGR-only vehicle exhibited homogeneous behaviour and had similar curves between different HES sets, with values ranging from ~75 °C to 212 °C and average 134.5 (sd. 12.6) °C.

Exhaust gas temperature and engine load values constrain the performance of exhaust gas aftertreatment systems. For the LNT vehicle, the highest emissions (HES-20) temperatures approximately corresponded to the rural and motorway sections, where engine load is high, thereby overgrowing LNT storage capacity. In this study, SCR exhibited high effectiveness in rural and motorway sections. Fig. 15, also shows that the SCR vehicle mainly reduced NO_x emissions for tailpipe exhaust gas temperatures of approximately 80–190 °C. Therefore, a low slope curve was observed for HES in this range. Observations above 190 °C show high NO_x emissions. This could be because SCR aftertreatment has an optimum internal operating temperature of approximately 300–400 °C [23], and it also requires an activation threshold temperature of ~200 °C [9]. SCR had relatively high urban emission factors. Depending on the HES set, it is observed that between 20 and 60% of high instantaneous emissions occurred at "low" exhaust gas temperatures (< 80 °C). Low temperatures are typical of urban traffic, along with idle and low engine loads [37,18]. Aftertreatment systems are affected by low internal temperatures when the engine is turned off by the stop-start system. In addition, they are also affected by high temperature exhaust gas during the regeneration process of the DPF, so thermal management of aftertreatment systems is an important research area. A practical solution to improve SCR performance was analysed in Jiang and Li [53] by controlling the transient temperature of an SCR system under European transient cycle (ETC). The excess of thermal energy was recovered to reach a regular target temperature of 288 °C. The SCR system showed an improved efficiency of more than 90%. There are a wide range of approaches to improve thermal management for catalytic converters, based on engine parameters on support devices and the performance of the catalyst [54].

In Fig. 16, although the exhaust gas temperatures of the RDE tests exhibit a high frequency at approximately 75 °C (grey area), all HES conditional distributions showed negative asymmetry. This means that HES observations are more likely to appear as the exhaust gas temperature increase, independent of the RDE test performed. The distributions of EGR and LNT vehicles show upward probabilities of HES observations over "low" exhaust gas temperatures of 75 °C. However, the SCR vehicle substantially increased the probability of high instantaneous emissions for exhaust gas temperatures over 150 °C, due to the DPF regeneration process.

The exhaust gas temperature and air-fuel equivalence ratio data used in this study are reference values, because they were measured at the tailpipe, and could vary for each vehicle model and PEMS installation. Moreover, the air-fuel equivalence ratio value is modified by chemical reactions downstream of the engine, mainly in the aftertreatment system, and the exhaust gas temperature depends on the physical conditions through the tailpipe and aftertreatment performance.

3.2.4. Engine speed

In relation to the engine speed values in RDE test, Fig. 17a shows great similarity in engine speed frequency distributions (grey area) for the three vehicles. All vehicles had the same engine speed modes. The urban driving section had three modes: Mo_{stop} ~ 0 rpm, Mo_{idle} ~ 800 rpm and Mo_{low} ~ 1600 rpm. The engines operated in the rural section in the vicinity of Mo_{low}, and the motorway section operated in the vicinity of Mo_{high} ~ 2200 rpm. This implies that all vehicles in running conditions ($v > 5\,km\,h^{-1}$) had two likely engine speed values of 1600 rpm for urban and rural sections, and 2200 rpm for the

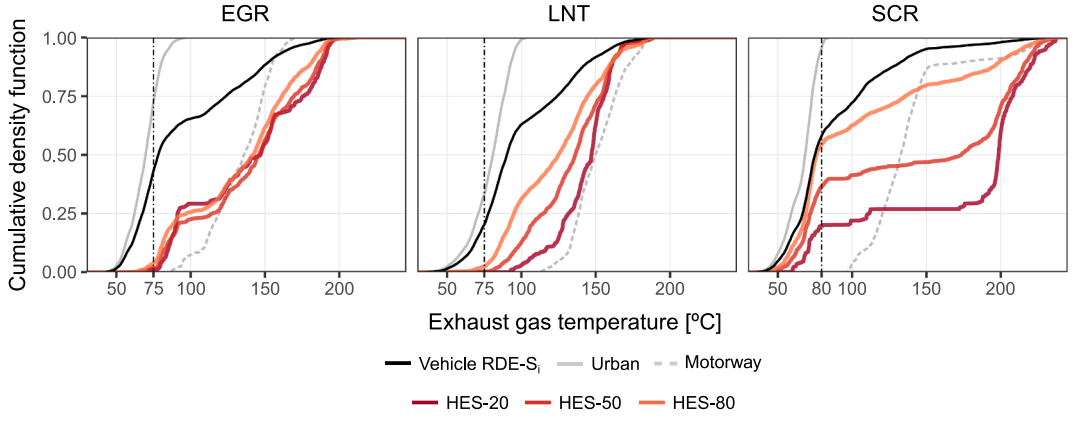

Fig. 15. Tailpipe exhaust gas temperature cumulative functions of high emissions sets (HES), RDE tests (RDE-S$_i$), urban and motorway sections.

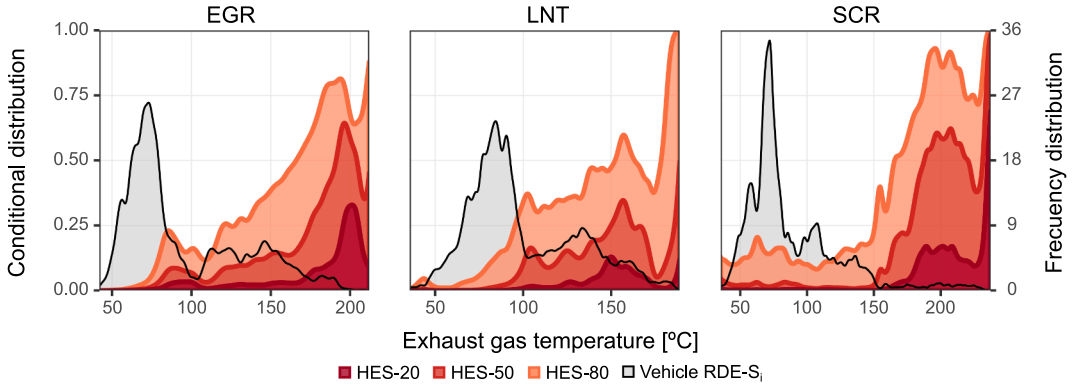

Fig. 16. Conditional probability of tailpipe exhaust gas temperature for high emission sets (HES) on the left axes. On the right axes, the grey area represents frequency distribution of RDE tests (RDE-S$_i$); normalized as RDE-S$_i$ = 1000 observations.

motorway section.

The engine speed frequency distribution of RDE tests influence the frequency distribution of HES observations. Moreover, the frequency distribution curves of HES (Fig. 17a) show than most high instantaneous emissions occurred between the Mo_{low} and Mo_{high} modes. Thus, high NO_x emissions are generated in a narrow range (~700 rpm) of engine speed operation. This range includes the maximum torque engine speed, where the flame temperature is usually high due to good combustion [52]. HES-20, HES-50 and HES-80 all exhibited similar curve shapes, but they differed in magnitude (number of observations). The Mo_{low} and Mo_{high} modes were close to the first and third quartiles for the entire RDE engine speed data. For each vehicle, these first-third quartile values resulted in: 1550–2200 rpm (EGR), 1650–2300 rpm (LNT) and 1500–2200 rpm (SCR).

Independent of engine speed RDE distribution, HES-80 conditional distribution with negative asymmetric distribution (in Fig. 17b) reflects the high probability of the occurrence of high instantaneous NO_x emissions as engine speed increases. The relationships between high engine speed, high engine load, driving severity and high NO_x emissions events show that high NO_x emissions are linked to engine operation parameters, which depends on the driving style [55]. This study shows that more severe driving, i.e. high engine speed and high $v{\cdot}a^+$, greatly increases the probability of high instantaneous NO_x emissions in real-world driving. This result is in agreement with the results obtained by Gallus et al. [27] where PEMS trips that involved an aggressive driving style increased NO_x emissions by 50–255% compared to normal driving style. In Franco et al. [22], second-by-second data showed that high $v{\cdot}a^+$ increases NO_x emissions by four times with respect to low $v{\cdot}a^+$. In Fonseca et al. [42], the computed performance index showed an increase of 50% for NO_x emissions due to aggressive driving

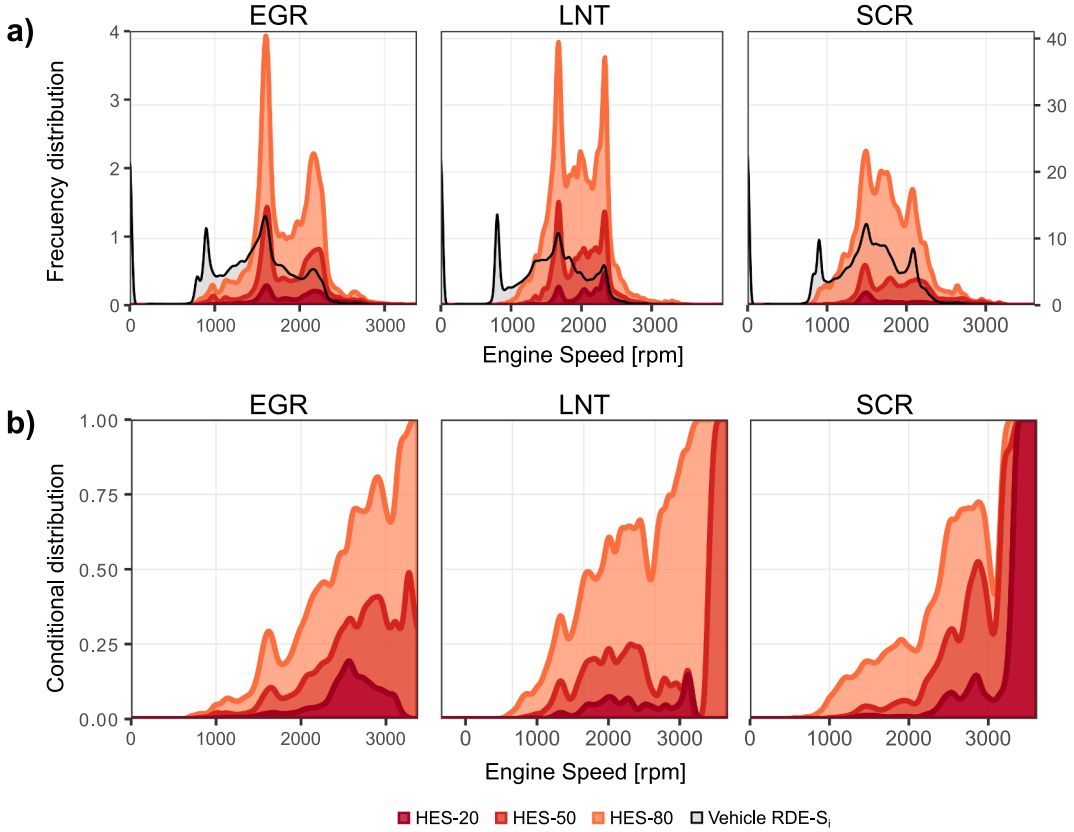

Fig. 17. Engine speed distributions (a) frequency distribution values of high emission sets (HES) on the left axes, and RDE tests (RDE-S$_i$) on the right axes. Frequency distributions are normalized, RDE-S$_i$ = 1000 observations (b) conditional probability of HES.

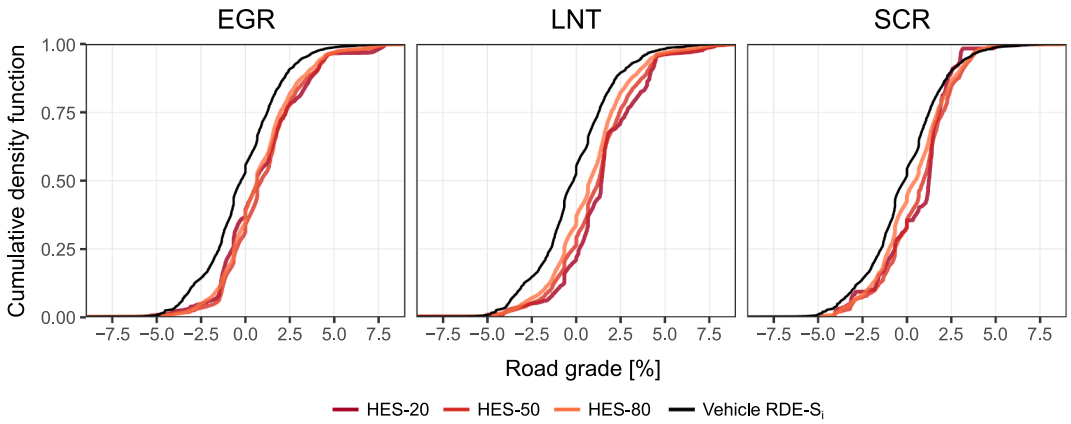

Fig. 18. Road grade cumulative functions of High emissions sets (HES) and RDE tests (RDE-S$_i$).

compared to normal driving of Euro 2–5 vehicles along an urban route. These results are not comparable because different approaches were adopted, but they are relevant to the findings of this study.

3.2.5. Road grade

The RDE route was approximately a closed loop, which means that there were equal positive and negative cumulative gains, as shown in the cumulative distributions of road grade for RDE tests in Fig. 18. However, 60–80% of HES observations were uphill (road grade > 0). Therefore, high instantaneous NO_x emissions are more likely to be produced on positive slopes due to higher engine load. Gallus et al. [27] also determined that NO_x emissions had a strong linear correlation with road grade, while Costagliola et al. [48] found a second order positive correlation between road grade and NO_x emissions in real-driving of rural sections. In Fig. 18, slopes less than −1.3% had relatively few HES observations for EGR and LNT vehicles due to fuel cut off and low engine load. The SCR vehicle reduced emissions in the entire range of possible values; therefore, their HES curves show a small difference compared to their RDE-S curve.

Strictly speaking, some of the numerical results of this study are limited to low-mileage vehicles of the same tested models. Literature shows that Euro 6 vehicles have a wide variability of NO_x emission levels; because, NO_x emissions depend on NO_x control technology and its configuration, management, usage time and maintenance [56]. However, the applied methodology used to classify HES and to analyse them, and the patterns identified in this study could be extrapolated to other diesel passenger vehicles at this time. Future studies could apply this methodology to a larger vehicle fleet, other routes, and broader boundary conditions. It is also possible to evaluate other aspects of the RDE test such as cold start.

4. Conclusions

Three Euro 6 diesel passenger cars equipped with the main NO_x control technologies were tested in an RDE test route, designed in the city of Madrid. A comprehensive analysis of the events of high instantaneous NO_x emissions (emission peaks) was performed. In the process, this study identified their high impact on emission factors and determined their relationships with vehicle speed, speed per positive acceleration ($v{\cdot}a^+$), air-fuel equivalence ratio (λ) at tailpipe, exhaust gas temperature, engine speed, and road grade. In addition, their probability of occurrence was determined. The main findings of this study lead to the following conclusions:

The instantaneous NO_x emissions of each vehicle were sorted and clustered in high emissions sets (HES). The contribution of these HES to real-world cumulated emissions showed the same patterns for all vehicles, and it led to the same conclusion: HES are composed of few observations with NO_x emission peaks, which means that high instantaneous NO_x emissions represent a large amount of cumulated emissions in a small amount of driving time. Although their theoretical constraint reduces emission factors by 30–82%, NO_x emissions in the entire range of operation sould be reduced to achieve Euro 6 real-world limits.

In relation to RDE tests, high instantaneous NO_x emissions are mainly generated in one modal speed value for each urban, rural and motorway sections. These speed modes mainly depend of road speed limits or RDE regulation. This suggests that hot spots in these operating conditions, could be identified and tackled by NO_x control systems and anti-pollution policies.

The SCR vehicle showed the potential to reduce NO_x emissions, thereby satisfying Euro 6d-TEMP NTE limits with a weighted deviation ratio of 1.1. This vehicle showed the best performance of the study in the motorway section, with a deviation ratio of 0.6. On the other hand, the worse-NO_x-reducers (EGR and LNT) vehicles did not meet NTE limits, showing weighted deviation ratios of 8.7 and 7.4, respectively. Their high instantaneous NO_x emissions were mainly produced in slightly lean mixture conditions ($1 \lesssim \lambda \lesssim 1.5$) and high exhaust gas temperature. These conditions that are indicative of high load were more frequent in motorway section than urban section. For the worse-NO_x-reducers of this study, these results are also explained by the shortcomings of their NO_x control technologies at high loads: limited recirculation of exhaust gas in EGR, and limited storage capacity in LNT systems.

The most frequent value of tailpipe exhaust gas temperature was 75 °C for all vehicles. For worse-NO_x-reducers (EGR and LNT) vehicles, almost all high instantaneous NO_x emissions were at “high” temperatures (over 75 °C). On the other hand, the SCR vehicle had almost all urban observations in match with up to 50% of high emissions at “low” exhaust gas temperatures (below 80 °C). This vehicle reduced the emission factors, but it had its relatively high emissions in the urban section, with a deviation ratio of 1.6. In this section, the SCR system is affected by low operating temperatures. Low operating temperatures of NO_x control systems are produced by stop-start periods and low exhaust gas flow in conditions of low speed driving and deceleration, which are typical conditions of urban driving and sometimes present in rural sections.

For the three tested vehicles, the high NO_x emissions were mainly produced in a narrow range of engine speeds (1500–2200 rpm). This range is between two noticeable engine speed modes and they were generated by the vehicles running in the entire RDE tests. Both modes were quantified by the first and third quartiles of the engine speed from RDE tests. This result could be similar for the three vehicles due to their similarity of powertrain, weight and dimensions.

Uphill, where a high engine load is required, showed larger probability to yield high instantaneous NO_x emissions. Between 60 and 80% of high instantaneous NO_x occurred uphill (road grade > 0).

Driving severity increases the probability of high NO_x emissions. The driving conditions with strong potential to generate HES observations are: $v{\cdot}a^+ > 9.2\,m^2\,s^{-3}$ (NEDC limit) and/or engine speed over 75th percentile of RDE observations. For worse-NO_x-reducers (EGR and LNT) vehicles, the conditions of elevated vehicle speed with hard acceleration (high $v{\cdot}a^+$) produced high NO_x emissions, particularly in rural and motorway sections. On the other hand, the relatively high NO_x emissions of SCR vehicle were also related to high $v{\cdot}a^+$ values; however, they matched with conditions of hard acceleration at low vehicle speed, particularly in urban and rural driving. Therefore, $v{\cdot}a^+$ is a robust indicator to assess and predict high instantaneous NO_x emissions. As such, speed reduction policies can lead to NO_x emissions reduction if they do not increase driving dynamics; namely, allowing fluid traffic with constant speed and limiting stops or hard accelerations.

High instantaneous NO_x emissions are produced in short time periods and are dependent of in-cylinder and aftertreatment operation; therefore, they are harder to identify and control. The methodology presented in this study identifies the conditions and probabilities required to find them so that this information could improve micro and meso emission models, which are based on data from engine and/or vehicle operating conditions. It could also help to predict the action of SCR systems to control ammonia injection. LNT systems and in-cylinder NO_x control technologies could take into account these findings to optimize their performance.

Declarations of interest

None.

Acknowledgments

The authors acknowledge Victor del Pozo, Nuria Flores and Bernardo Martínez at the University Institute for Automobile Research (INSIA), Universidad Politécnica de Madrid (UPM) for their help with the experimental part of this study.

Appendix A. Supplementary material

Supplementary data related to this article can be found at https://doi.org/10.1016/j.apenergy.2019.03.120.

References

[1] Jonson JE, Borken-Kleefeld J, Simpson D, Nyíri A, Posch M, Heyes C. Impact of excess NO_x emissions from diesel cars on air quality, public health and eutrophication in Europe. Environ Res Lett 2017;12(9):094017. https://doi.org/10.1088/1748-9326/aa8850.

[2] EEA. Exceedance of air quality limit values in urban areas (CSI 004); 2015. Retrieved May 29, 2018, from < https://www.eea.europa.eu/data-and-maps/indicators/exceedance-of-air-quality-limit-3/assessment-3 > .

[3] EEA. Emissions of air pollutants from transport; 2017. Retrieved May 29, 2018, from < https://www.eea.europa.eu/data-and-maps/indicators/transport-emissions-of-air-pollutants-8/transport-emissions-of-air-pollutants-5 > .

[4] EEA. Size of the vehicle fleet; 2017. Retrieved May 29, 2018, from < https://www.eea.europa.eu/data-and-maps/indicators/size-of-the-vehicle-fleet/size-of-the-vehicle-fleet-8 > .

[5] ICCT. European vehicle market statistics; 2016. Pocketbook 2017/18. Retrieved from < http://www.eafo.eu/content/european-vehicle-categories > .

[6] Carslaw DC, Beevers SD, Tate JE, Westmoreland EJ, Williams ML. Recent evidence concerning higher NO_x emissions from passenger cars and light duty vehicles. Atmos Environ 2011;45(39):7053–63. https://doi.org/10.1016/j.atmosenv.2011.09.063.

[7] Hooftman N, Messagie M, Van Mierlo J, Coosemans T. A review of the European passenger car regulations – real driving emissions vs local air quality. Renew Sustain Energy Rev 2018;86(March 2017):1–21. https://doi.org/10.1016/j.rser.2018.01.012.

[8] Franco V, Kousoulidou M, Muntean M, Ntziachristos L, Hausberger S, Dilara P. Road vehicle emission factors development: a review. Atmos Environ 2013;70:84–97. https://doi.org/10.1016/j.atmosenv.2013.01.006.

[9] Ntziachristos L, Papadimitriou G, Ligterink N, Hausberger S. Implications of diesel emissions control failures to emission factors and road transport NO_x evolution. Atmos Environ 2016;141:542–51. https://doi.org/10.1016/j.atmosenv.2016.07.036.

[10] EC. Commission Regulation (EU) 2016/646 of 20 April 2016 amending Regulation (EC) No 692/2008 as regards emissions from light passenger and commercial vehicles (Euro 6). II Official Journal of the European Union 20–30; 2016. Retrieved from < http://data.europa.eu/eli/reg/2016/646/oj > .

[11] EC. Commission Regulation (EU) 2016/427 of 10 March 2016 amending Regulation (EC) No 692/2008 as regards emissions from light passenger and commercial vehicles (Euro 6). Off J Eur Union; 2016. Retrieved from < https://eur-lex.europa.eu/eli/reg/2016/427/oj > .

[12] EC. Commission Regulation (EU) 2017/1151 of 1 June 2017 supplementing Regulation (EC) No 715/2007 of the European Parliament and of the Council on type-approval of motor vehicles with respect to emissions from light passenger and commercial vehicles (Euro 5 a (2017)). Retrieved from < http://data.europa.eu/eli/reg/2017/1151/oj > .

[13] Millo F, Giacominetto PF, Bernardi MG. Analysis of different exhaust gas recirculation architectures for passenger car Diesel engines. Appl Energy 2012;98:79–91. https://doi.org/10.1016/j.apenergy.2012.02.081.

[14] Thangaraja J, Kannan C. Effect of exhaust gas recirculation on advanced diesel combustion and alternate fuels – a review. Appl Energy 2016;180:169–84. https://doi.org/10.1016/j.apenergy.2016.07.096.

[15] Johnson TV. Review of vehicular emissions trends. SAE Int J Engines 2015;8(3):1152–67. https://doi.org/10.4271/2015-01-0993.

[16] Ko J, Jin D, Jang W, Myung CL, Kwon S, Park S. Comparative investigation of NO_x emission characteristics from a Euro 6-compliant diesel passenger car over the NEDC and WLTC at various ambient temperatures. Appl Energy 2017;187(x):652–62. https://doi.org/10.1016/j.apenergy.2016.11.105.

[17] Myung CL, Jang W, Kwon S, Ko J, Jin D, Park S. Evaluation of the real-time de-NO performance characteristics of a LNT-equipped Euro-6 diesel passenger car with various vehicle emissions certification cycles. Energy 2017;132(x):356–69. https://doi.org/10.1016/j.energy.2017.05.089.

[18] Yang L, Vicente F, Alex C, John G, Peter M. NO_x control technologies for Euro 6 diesel passenger cars: market penetration and experimental performance assessment (white paper). Washington: International Council on Clean Transportation; 2015.

[19] Reşitoılu IA, Altinişik K, Keskin A. The pollutant emissions from diesel-engine vehicles and exhaust aftertreatment systems. Clean Technol Environ Policy 2015;17(1):15–27. https://doi.org/10.1007/s10098-014-0793-9.

[20] Sanchez FP, Bandivadekar A, German J. Estimated cost of emission reduction technologies for LDVs. The International Council on Clean Transportation; 2012. Retrieved from < http://www.theicct.org/estimated-cost-emission-reduction-technologies-ldvs > .

[21] Sandhu GS, Frey HC, Bartelt-Hunt S, Jones E. Real-world activity, fuel use, and emissions of diesel side-loader refuse trucks. Atmos Environ 2016;129:98–104. https://doi.org/10.1016/j.atmosenv.2016.01.014.

[22] Franco V, Posada Sánchez F, German J, Mock P. Real-world exhaust emissions from modern diesel cars. A meta-analysis of PEMS emissions data from EU (Euro 6) and US (Tier 2 Bin 5/ULEV II) diesel passenger cars. Part 1: aggregated results [White Paper]. The International Council On Clean Transportation (October), vol. 59; 2014. Retrieved from < http://www.theicct.org/sites/default/files/publications/ICCT_PEMS-study_diesel-cars_20141010.pdf > .

[23] Yang L, Franco V, Mock P, Kolke R, Zhang S, Wu Y, et al. Experimental assessment of NO_x emissions from 73 Euro 6 diesel passenger cars. Environ Sci Technol 2015;49(24):14409–15. https://doi.org/10.1021/acs.est.5b04242.

[24] O'Driscoll R, ApSimon HM, Oxley T, Molden N, Stettler MEJ, Thiyagarajah A. A portable emissions measurement system (PEMS) study of NO_x and primary NO_2 emissions from Euro 6 diesel passenger cars and comparison with COPERT emission factors. Atmos Environ 2016;145(2):81–91. https://doi.org/10.1016/j.atmosenv.2016.09.021.

[25] Degraeuwe B, Weiss M. Does the New European Driving Cycle (NEDC) really fail to capture the NO_x emissions of diesel cars in Europe? Environ Pollut 2017;222(X):234–41. https://doi.org/10.1016/j.envpol.2016.12.050.

[26] Luján JM, Bermúdez V, Dolz V, Monsalve-Serrano J. An assessment of the real-world driving gaseous emissions from a Euro 6 light-duty diesel vehicle using a portable emissions measurement system (PEMS). Atmosp Environ 2018;174(November 2017):112–21. https://doi.org/10.1016/j.atmosenv.2017.11.056.

[27] Gallus J, Kirchner U, Vogt R, Benter T. Impact of driving style and road grade on gaseous exhaust emissions of passenger vehicles measured by a Portable Emission Measurement System (PEMS). Transp Res Part D: Transp Environ 2017;52(2):215–26. https://doi.org/10.1016/j.trd.2017.03.011.

[28] Kwon S, Park Y, Park J, Kim J, Choi KH, Cha JS. Characteristics of on-road NO_x emissions from Euro 6 light-duty diesel vehicles using a portable emissions measurement system. Sci Total Environ 2017;576(x):70–7. https://doi.org/10.1016/j.scitotenv.2016.10.101.

[29] O'Driscoll R, Stettler MEJ, Molden N, Oxley T, ApSimon HM. Real world CO2 and NO_x emissions from 149 Euro 5 and 6 diesel, gasoline and hybrid passenger cars. Sci Total Environ 2018;621(x):282–90. https://doi.org/10.1016/j.scitotenv.2017.11.271.

[30] Cha J, Lee J, Chon MS. Evaluation of real driving emissions for Euro 6 light-duty diesel vehicles equipped with LNT and SCR on domestic sales in Korea. Atmos Environ 2019;196:133–42. https://doi.org/10.1016/j.atmosenv.2018.09.029.

[31] Chong HS, Park Y, Kwon S, Hong Y. Analysis of real driving gaseous emissions from light-duty diesel vehicles. Transp Res Part D: Transp Environ 2018;65(October):485–99. https://doi.org/10.1016/J.TRD.2018.09.015.

[32] Wang H, Ge Y, Hao L, Xu X, Tan J, Li J, et al. The real driving emission characteristics of light-duty diesel vehicle at various altitudes. Atmos Environ

2018;191(July):126–31. https://doi.org/10.1016/j.atmosenv.2018.07.060.
[33] Triantafyllopoulos G, Katsaounis D, Karamitros D, Ntziachristos L, Samaras Z. Experimental assessment of the potential to decrease diesel NO emissions beyond minimum requirements for Euro 6 Real Drive Emissions (RDE) compliance. Sci Total Environ 2018;618(x):1400–7. https://doi.org/10.1016/j.scitotenv.2017.09.274.
[34] Fonseca González NE. Aspectos de la medición dinámica instantánea de emisiones de motores. Aplicación al desarrollo de un equipo portátil y una metodología para estudios de contaminación de vehículos en tráfico real. Universidad Politécnica de Madrid; 2012https://doi.org/10.20868/UPM.thesis.14269.
[35] Fonseca González N, Casanova Kindelán J, López Martínez JM. Methodology for instantaneous average exhaust gas mass flow rate measurement. Flow Meas Instrum 2016;49(April):52–62. https://doi.org/10.1016/j.flowmeasinst.2016.04.007.
[36] Weiss M, Bonnel P, Kühlwein J, Provenza A, Lambrecht U, Alessandrini S, et al. Will Euro 6 reduce the NO_x emissions of new diesel cars? - Insights from on-road tests with Portable Emissions Measurement Systems (PEMS). Atmos Environ 2012;62(2):657–65. https://doi.org/10.1016/j.atmosenv.2012.08.056.
[37] Weiss M, Bonnel P, Hummel R, Provenza A, Manfredi U. On-road emissions of light-duty vehicles in Europe. Environ Sci Technol 2011;45(19):8575–81. https://doi.org/10.1021/es2008424.
[38] Thompson GJ, Carder DK, Besch MC, Thiruvengadam A, Kappanna HK. In-use emissions testing of light-duty diesel vehicles in the United States; 2014.
[39] Weiss M, Bonnel P, Hummel R, Manfredi U, Colombo R, Lanappe G, et al. Analyzing on-road emissions of light-duty vehicles with Portable Emission Measurement Systems (PEMS). European Commission Joint Research Centre Technical Report EUR 24697 EN. JCR; 2011.
[40] D'Ambrosio S, Finesso R, Fu L, Mittica A, Spessa E. A control-oriented real-time semi-empirical model for the prediction of NO_x emissions in diesel engines. Appl Energy 2014;130:265–79. https://doi.org/10.1016/j.apenergy.2014.05.046.
[41] Finesso R, Spessa E. A real time zero-dimensional diagnostic model for the calculation of in-cylinder temperatures, HRR and nitrogen oxides in diesel engines. Energy Convers Manage 2014;79:498–510. https://doi.org/10.1016/j.enconman.2013.12.045.
[42] Fonseca González N, Casanova Kindelán J, Espinosa Zapata F. Influence of driving style on fuel consumption and emissions in diesel- powered passenger car. 18th international symposium transport and air pollution. 2010. p. 1–6.
[43] Venables WN, Ripley BD. Modern applied statistics with S vol. 4. New York (NY): Springer New York; 2002https://doi.org/10.1007/978-0-387-21706-2.
[44] Heijne V, Ligterink N, Stelwagen U. 2016 Emission factors for diesel Euro-6 passenger cars, light commercial vehicles and Euro-VI trucks; 2016. https://doi.org/10.13140/RG.2.1.3608.7922.
[45] May J, Favre C, Bosteels D, Andersson J, Clarke D, Heaney M. On-road testing and PEMS data analysis for two Euro 6 diesel vehicles. 20th international transport and air pollution conference 2014. 2014. p. 1–6.
[46] Elvik R. A restatement of the case for speed limits. Transp Policy 2010;17(3):196–204. https://doi.org/10.1016/j.tranpol.2009.12.006.
[47] Elvik R. A review of game-theoretic models of road user behaviour. Accid Anal Prev 2014;62:388–96. https://doi.org/10.1016/j.aap.2013.06.016.
[48] Costagliola MA, Costabile M, Prati MV. Impact of road grade on real driving emissions from two Euro 5 diesel vehicles. Appl Energy 2018;231(July):586–93. https://doi.org/10.1016/j.apenergy.2018.09.108.
[49] Zeldovich Y, Sadovnikov P, Kamenetskii D. Oxidation of nitrogen in combustion. [(Translation by M. Shelef), Ed.]. Moscow-Leningrad: Academy of Sciences of USSR, Institute of Chemical Physics; 1947.
[50] Guardiola C, Martín J, Pla B, Bares P. Cycle by cycle NO model for diesel engine control. Appl Therm Eng 2017;110:1–2. https://doi.org/10.1016/j.applthermaleng.2016.08.170.
[51] Carslaw DC, Williams ML, Tate JE, Beevers SD. The importance of high vehicle power for passenger car emissions. Atmos Environ 2013;68:8–16. https://doi.org/10.1016/j.atmosenv.2012.11.033.
[52] Heywood JB. Internal combustion engine fundamentals. McGrawHill series in mechanical engineering vol. 21. McGraw-Hill; 1988https://doi.org/10987654.
[53] Jiang J, Li D. Theoretical analysis and experimental confirmation of exhaust temperature control for diesel vehicle NO_x emissions reduction. Appl Energy 2016;174:232–44. https://doi.org/10.1016/j.apenergy.2016.04.096.
[54] Gao J, Tian G, Sorniotti A, Karci AE, Di Palo R. Review of thermal management of catalytic converters to decrease engine emissions during cold start and warm up. Appl Therm Eng 2019. https://doi.org/10.1016/j.applthermaleng.2018.10.037.
[55] Casanova Kindelán J, Fonseca González N, Espinosa Zapata F. Proposal of a dynamic performance index to analyze driving pattern effect on car emissions. Actes INRETS N° 122 (2002); 2009. p. 1–9. Retrieved from < oa.upm.es/13475/1/INVE_MEM_2009_78672.pdf > .
[56] Lee T, Shin M, Lee B, Chung J, Kim D, Keel J, et al. Rethinking NO_x emission factors considering on-road driving with malfunctioning emission control systems: a case study of Korean Euro 4 light-duty diesel vehicles. Atmos Environ 2019;202(x):212–22. https://doi.org/10.1016/j.atmosenv.2019.01.032.
[57] Zhu D, Zheng X. Asymmetric twin-scroll turbocharging in diesel engines for energy and emission improvement. Energy 2017;141(x):702–14. https://doi.org/10.1016/j.energy.2017.07.173.
[58] Zhu D, Zheng X. Fuel consumption and emission characteristics in asymmetric twin-scroll turbocharged diesel engine with two exhaust gas recirculation circuits. Appl Energy 2019;238(January):985–95. https://doi.org/10.1016/j.apenergy.2019.01.188.